Tetrahedron 67 (2011) 125–143

Contents lists available at ScienceDirect

Tetrahedron

journal homepage: www.elsevier.com/locate/tet

OPE/OPV H-mers: synthesis, electronic properties, and spectroscopic responses to binding with transition metal ions

Ningzhang Zhou, Li Wang, David W. Thompson, Yuming Zhao *

Department of Chemistry, Memorial University of Newfoundland, St. John's, Newfoundland, Canada A1B 3X7

ARTICLE INFO

Article history:
Received 25 August 2010
Received in revised form 1 November 2010
Accepted 2 November 2010
Available online 5 November 2010

Keywords:
Oligomer
Electronic substitution
Sonogashira coupling
HWE reaction
Chemosensor

ABSTRACT

A new type of structurally defined H-shaped OPE/OPV co-oligomers (termed H-mers) functionalized with various donor and/or acceptor end groups was synthesized by iterative Sonogashira coupling and Horner–Wadsworth–Emmons (HWE) reactions. Electronic substitution effects on the H-mer backbone were investigated by UV–vis absorption and fluorescence spectroscopy. Some H-mers were found to show spectral responses upon binding to an acid (TFA) or transition metal ions, revealing the applicability of H-mers in the field of chromophore and fluorophore based chemosensors.

1. Introduction

The extensive studies on monodisperse and structurally defined π-conjugated oligomers over the past few decades have not only allowed the complex structure–property relationships for related polymeric materials to be well understood, but also led to an enormous array of oligomer and polymer-based materials useful for advanced molecular electronic and optoelectronic applications.[1–9] While the straightforward linearly π-conjugated architecture still remains a popular design motif in the current π-oligomer family,[7,10–12] a surging interest in constructing oligomers with various 2-dimensional noncyclic π-frameworks has become notable in recent years.[13–17] A major rationale for pursuing such complex structures lies in the opportunities of obtaining some unique physical and electronic properties unattainable from linearly conjugated oligomers. For instance, the steric bulkiness of dendritic and branched π-oligomers has been proven effective at improving solubility (processability) and optimizing π–π aggregation for better optoelectronic and semi-conducting properties.[18–26] The relatively rigid molecular structures of 2-dimensional π-oligomers serve nanoscale scaffolds for the construction of well-defined molecular optoelectronic and mechanical devices.[23,27–45] The spatially non-overlapping frontier molecular orbitals (FMOs) of 2-dimensional cruciform-shaped π-oligomers have enabled the design of functional organic chromo-/fluorophores to attain remarkable molecular sensor performance.[46–52]

Three basic structural themes can be generalized from the numerous 2-dimensional conjugated oligomers so far reported in the literature according to their molecular shapes; X, Y, and H-shaped assemblages (henceforth referred to as X-mers, Y-mers, and H-mers, respectively). Fig. 1 lists the representative core structures of some 2-dimensional conjugated phenylene-based oligomer scaffolds. A large number of oligomers derived from the backbones of X-mers (also known as cruciforms)[19,39,53–62] and Y-mers (sometimes termed star-shaped oligomers)[25,26,36,42,44,63–84] has been synthesized and characterized in recent studies. In contrast, the number of H-mers existing in the literature still remains relatively small mainly because of their demanding and tedious synthesis.[31,36,37,59,85–87]

Structurally, the distinction between H-mers and other 2-dimensional oligomers (X-mers and Y-mers) is that the pivotal segment of an H-mer is made up of a linear oligomeric moiety instead of a monomeric unit, such as a single atom, arene or vinyl group, etc. As such, the H-mers are predicted to show combined properties stemming from conjugated and cross-conjugated π-electron delocalization patterns as well as unique inter-oligomer π–π interactions. Moreover, the H-shaped topology allows more flexibly terminal functionalization on the oligomer framework such that better control over electronic and physical properties can be exerted at the molecular level. Such features should in turn render the H-mer an appealing platform for the design of new oligomer and polymer functional nanomaterials.[9,36,59,85–87] In light of the paucity

* Corresponding author. Tel.: +1 709 864 8747; fax: +1 709 864 3702; e-mail address: yuming@mun.ca (Y. Zhao).

0040-4020/$ – see front matter © 2010 Elsevier Ltd. All rights reserved.
doi:10.1016/j.tet.2010.11.012

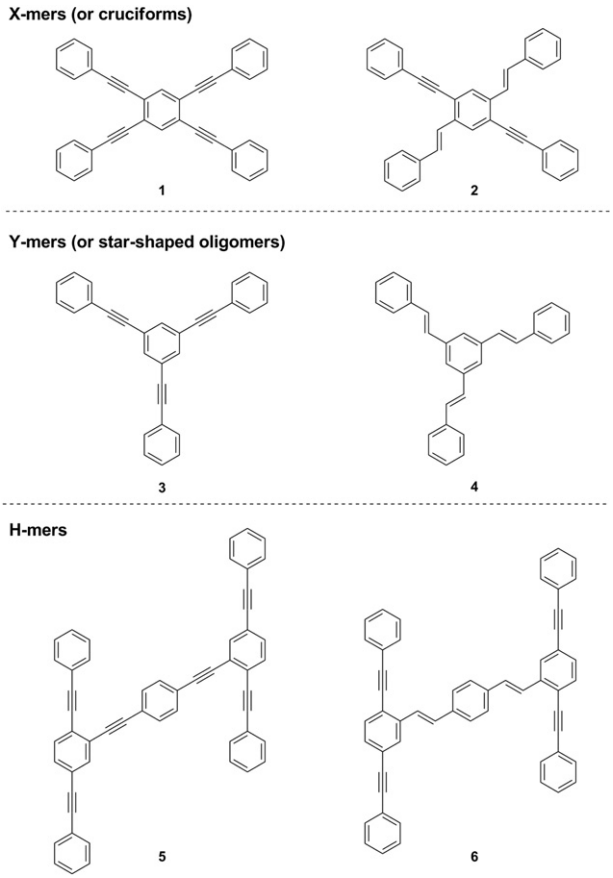

Fig. 1. Representative core structures for phenylene-based X-mers, Y-mers, and H-mers.

of synthetic examples and fundamental understanding of H-mers in the current literature, we recently set out a systematic survey on a class of H-mers that hybridize linear oligo(phenylene ethynylene) (OPE) and oligo(phenylene vinylene) (OPV) motifs as shown in structure **6** (Fig. 1). In a preceding report, we have explored the donor/acceptor (D/A) substitution effects on the UV–vis absorption and fluorescence properties of some OPE/OPV H-mers and demonstrated that upon functionalization with amino groups at the terminal positions, the H-mer could give rise to efficient fluorescence sensing function towards acids and transition metal ions.[85] This article outlines our detailed studies on this type of H-mers in a broader context, including efficient synthetic methods, structure–property relationship, electronic substitution effects, UV–vis, and fluorescence spectroscopic responses to acid and various metal cations.

2. Synthesis of OPE/OPV H-mers

2.1. Synthesis of short OPE/OPV H-mers

To construct OPE/OPV H-mers, an OPV building block **14** had to be acquired beforehand as the central pivotal bridge. As shown in Scheme 1, 2-aminobenzoic acid (**7**) was brominated with Br_2 to give 2-amino-5-bromobenzoic acid (**8**). Compound **8** underwent a diazotization reaction followed by treatment with KI to afford 5-bromo-2-iodobenzoic acid (**9**), which was then subjected to a Fischer esterification with MeOH in the presence of concd H_2SO_4 to yield methyl benzoate **10**. Compound **10** was further reduced into benzyl alcohol **11** by diisobutylaluminum hydride (DIBAL). Oxidation of **11** with pyridinium dichromate (PDC) resulted in the formation of 5-

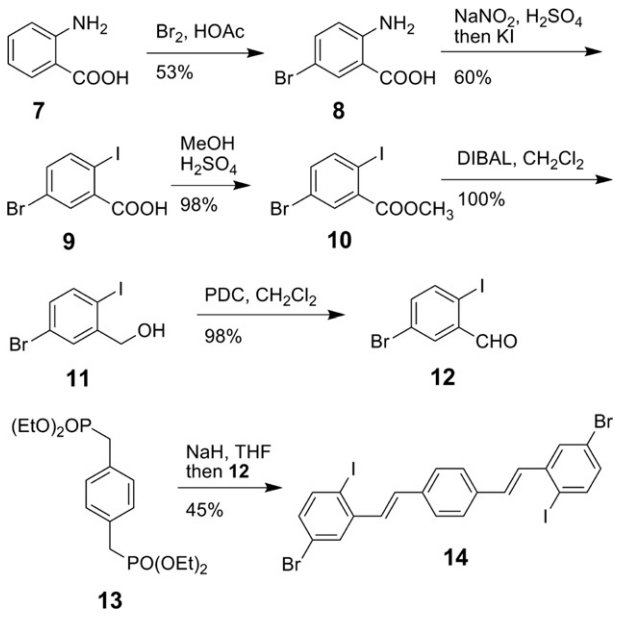

Scheme 1. Synthesis of OPV precursor **14**.

bromo-2-iodobenzaldehyde (**12**) in a nearly quantitative yield. Compound **12** was subjected to a Horner–Wadsworth–Emmons (HWE) reaction with the phosphonate ylide generated by treating bis(phosphonate) **13** with NaH, affording the desired dibromo-diiodo-OPV precursor **14** in a reasonable yield of 45%.

OPV precursor **14** was subjected to Sonogashira coupling with excess trimethylsilylacetylene (TMSA) catalyzed by $Pd(PPh_3)_2Cl_2$ and CuI in the presence of Et_3N as base to afford tetraalkynyl OPV **15** (Scheme 2). Removal of the TMS groups in compound **15** by K_2CO_3 at rt resulted in free terminal alkyne **16** in a quantitative yield. Compound **16** then underwent a four-fold Sonogashira coupling with iodobenzene to yield unsubstituted short H-mer **17** in 67% yield. In a similar manner, two D/A/substituted short H-mers, **18** and **19**, were synthesized via the Sonogashira coupling approach. In these two H-mers, the terminal phenyl rings were, respectively, functionalized with electron-donating $-NMe_2$ and electron-withdrawing –COOMe groups to serve as models for probing the D/A-substitution effects on the π-electronic properties of short H-mers.

It is worth noting that the Sonogashira (alkynyl coupling) approach as demonstrated in Scheme 2 turned out to be very efficient in constructing D/A-substituted short OPE/OPV H-mers. On the other hand, the synthetic strategy involving olefination at the last stage of the H-mer backbone assemblage is also conceivably plausible. To explore the effectiveness of this alternative synthetic route, the synthesis of functionalized H-mer **18** was attempted via an olefination reaction between phosphonate **13** and OPE-aldehyde **22** in the presence of base (Scheme 3). Unfortunately, despite numerous conditions tried out (with different bases and solvents), the HWE reaction did not afford the desirable H-mer product in meaningful yield. In most cases, the reaction ended with either significant decomposition of the OPE-aldehyde precursor or a mixture of multiple intractable side products. These findings thus suggest that the HWE reaction is not suited to be placed at the final step in planning the synthesis of short OPE/OPV H-mers.

To evaluate the electron 'push–pull' effect,[7] a D/A-substituted H-mer OPE/OPV **29** (Scheme 4) was targeted (note that D/A herein refers to 'donor and acceptor', while D/A denotes 'donor or acceptor'). In terms of synthetic efficiency, the convergent strategy of merging two pre-assembled D/A-substituted OPE precursors by HWE reaction was deemed concise and preferable for this type of H-mers, although the HWE reaction failed in obtaining A-substituted H-mer

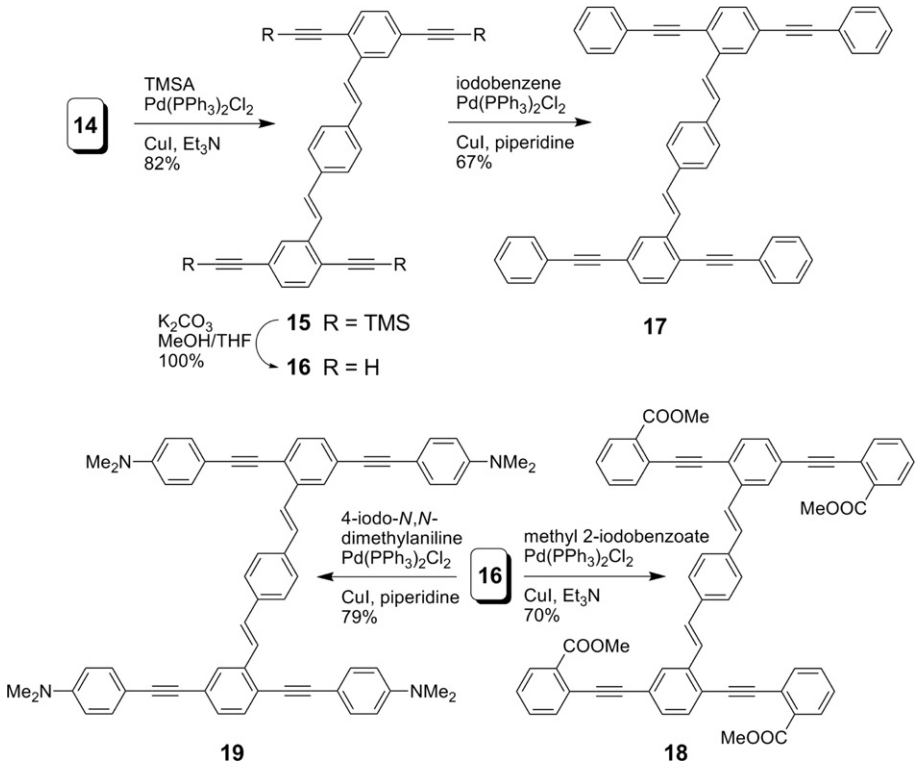

Scheme 2. Synthesis of short OPE/OPV H-mers **17**–**19** by Sonogashira coupling.

18 previously. As depicted in Scheme 4, the iodo group of compound **12** was first converted into an alkynyl group by reacting with 1 M equiv of triisopropylsilylacetylene (TIPSA) under Sonogashira conditions to give **23** in 94% yield. Another step of Sonogashira coupling between **23** and TMSA afforded **24** in a high yield. Selective removal of the TMS group in **24** with K_2CO_3 led to compound **25**, which was then cross-coupled with methyl 2-iodobenzoate to yield phenylacetylene dimer **26**. Desilylation of **26** with tetrabutylammonium fluoride (TBAF) followed by cross coupling with 4-iodo-*N*,*N*-dimethylaniline afforded OPE precursor **28** in a moderate yield of 47%. At this juncture, it would only require one more step of HWE reaction to accomplish the construction of D/A functionalized H-mer **29**. Nevertheless, problematic outcomes of the HWE reaction similar to those encountered in Scheme 3 emerged and hence forced us to abandon this synthetic route.

Alternatively, the synthesis of D/A-substituted H-mer **29** by a relatively lengthier iterative Sonogashira coupling route was investigated. As shown in Scheme 5, phosphonate **13** was first deprotonated by NaH in THF to generate a ylide intermediate, which was immediately reacted with aldehyde **23** to form OPV **30** in 45% yield over two steps. Compound **30** was cross-coupled with 2 M equiv of TMSA under Sonogashira conditions to afford tetraalkynylated OPV **31**. Selective deprotection of the TMS groups in **31** by K_2CO_3 then yielded free terminal alkyne **32**. Cross coupling of **32** with methyl

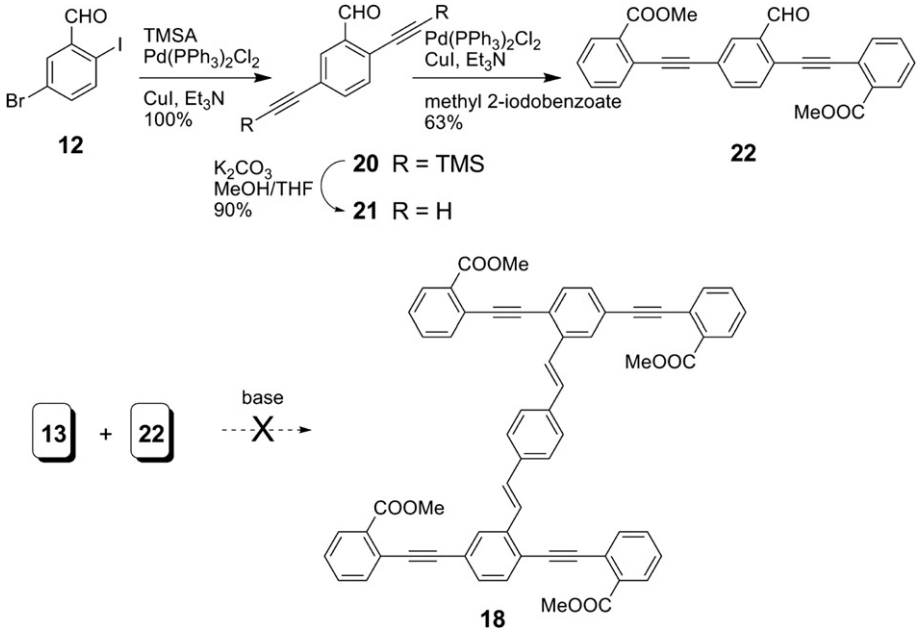

Scheme 3. Attempted synthesis of short OPE/OPV H-mer **18** by HWE reaction.

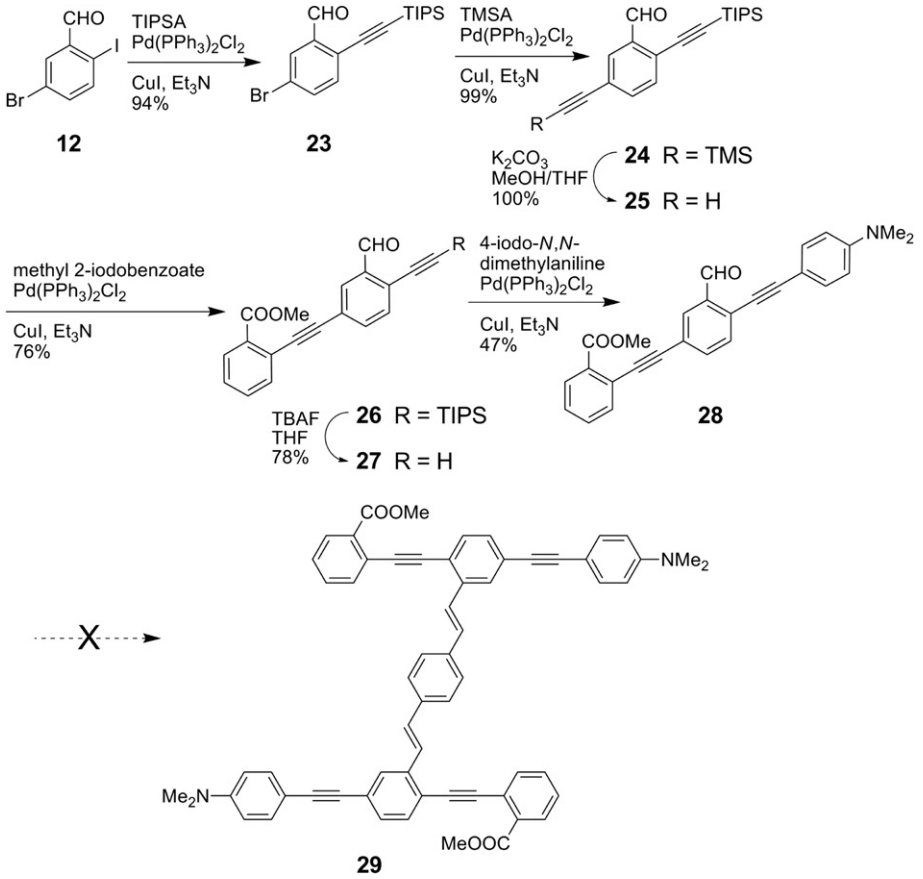

Scheme 4. Attempted synthesis of D/A substituted short OPE/OPV H-mer **29** by HWE reaction.

2-iodobenzoate under the catalysis of Pd/Cu gave oligomer **33** in a decent yield. Finally, desilylation of **33** with TBAF, followed by cross coupling with 4-iodo-*N*,*N*-dimethylaniline, successfully led to the formation of D/A-substituted short H-mer **29**. It should be noted that in the last cross-coupling step involving 4-iodo-*N*,*N*-dimethylaniline and terminal alkynes, the use of piperidine as base resulted in a much higher yield than the commonly used base Et_3N.

2.2. Synthesis of long OPE/OPV H-mers

At this point, short H-mers with various types of end groups have been obtained. To investigate the effect of π-conjugation length on related molecular properties, a set of H-mers with relatively longer OPE branches was subsequently targeted. The synthesis of unsubstituted long OPE/OPV H-mer was readily achieved by a four-fold Sonogashira coupling between iodoarene **35** and OPV precursor **16** as shown in Scheme 6. The relatively low yield of this reaction (36%) compared with previous cross coupling reactions was ascribed to the occurrence of some undesirable homocoupling side-reactions as well as mechanical loss during column chromatographic separation due to the high viscosity of the compound.

To synthesize D/A-substituted long OPE/OPV H-mers, the strategy of employing Sonogashira coupling to construct the H-mer skeleton at the final stage of synthesis was planned and investigated. Two phenylacetylene dimers **41** and **46**, end-substituted with a donor (OMe) or acceptor (CN) group in each, were first prepared as shown in Scheme 7. A commercially available benzene derivative, 4-bromobenzonitrile (**37**), was converted into **38** via Sonogashira coupling with TMSA. Desilylation of **38** with K_2CO_3 followed by another Sonogashira coupling with iodoarene **35** gave compound **40**, which was readily desilylated with K_2CO_3 to afford cyano-substituted phenylacetylene dimer **41** in a good yield. By a similar synthetic route, methoxy end-substituted dimer **46** was acquired from 4-iodoanisole (**42**) through four synthetic steps as outlined in Scheme 7.

With precursors **41** and **46** in hand, two D/A-substituted long OPE/OPV H-mers, **47** and **48** were synthesized in reasonable yields by a four-fold Sonogashira coupling reaction as illustrated in Scheme 8. In a similar manner, an aldehyde end-substituted phenylacetylene dimer **49** was cross-coupled with OPV precursor **14** to afford another A-substituted long H-mer **50** in 68% yield. Note that the yields of these coupling reactions were comparatively greater than that of H-mer **36** (Scheme 6). This can be attributed to the presence of D/A end groups in the phenylene ethynylene branches, which activate the reactivity of terminal alkyne.

In contrast to the attempted synthesis of short H-mer **29** (Scheme 4), the synthesis of D/A-substituted long OPE/OPV H-mers by a convergent HWE strategy met with success. This synthetic route began with the preparation of two D/A-substituted phenylacetylene pentamers **52** and **54** via iterative Sonogashira reactions (Scheme 9). Note that the two OPE precursors are regio-isomers to one another (vide infra), resulting from different coupling sequences. The central phenyl ring of **52** and **54** was functionalized with an aldehyde group to enable the assembly of respective H-mers **55** and **56** via an HWE reaction with the phosphonate ylide of **13** (Scheme 10) in satisfactory yields.

Finally, the synthesis of another D/A-substituted long OPE/OPV H-mer **58** was carried out via a convergent Sonogashira coupling approach outlined in Scheme 11. In this route, the iodo groups of OPV precursor **14** were first selectively cross-coupled with 2 M equiv of phenylacetylene dimer **46** to yield a Z-shaped OPE/OPV co-oligomer **57** in a reasonable yield. Another iteration of two-fold Sonogashira coupling between **57** and phenylacetylene dimer **49** thus gave D/A-substituted long H-mer **58** in 61% yield.

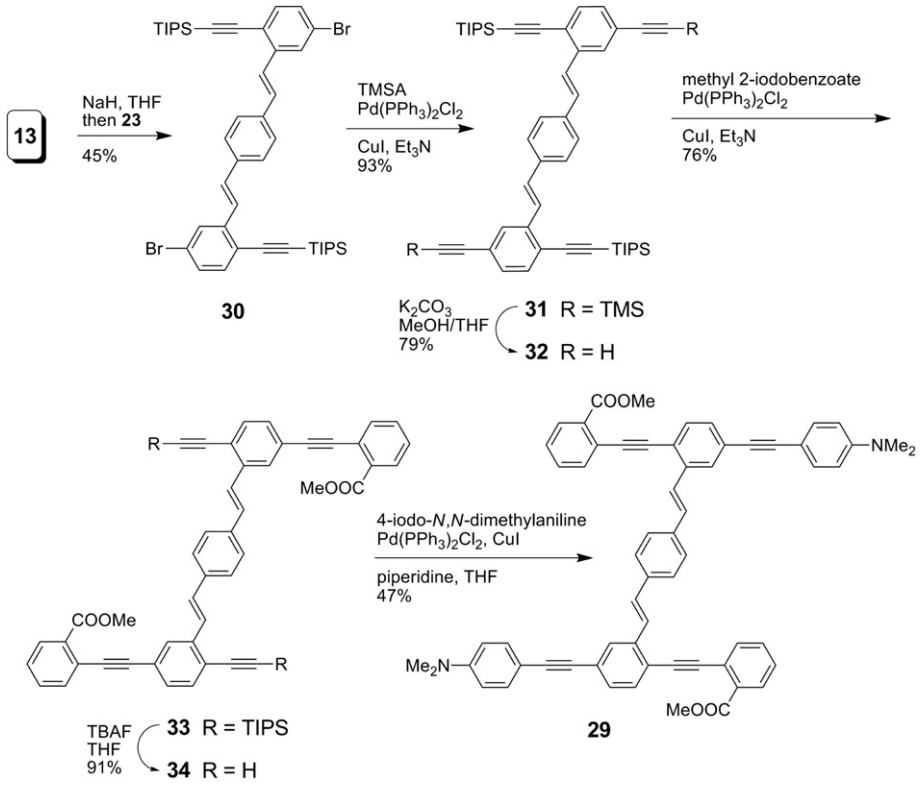

Scheme 5. Synthesis of D/A substituted short OPE/OPV H-mer **29** by Sonogashira coupling.

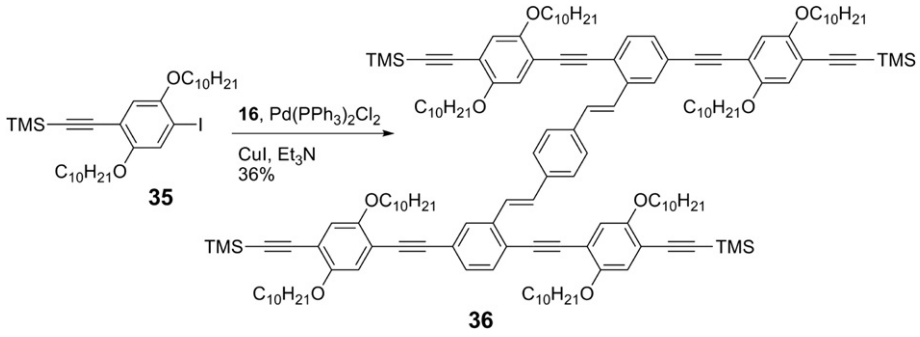

Scheme 6. Synthesis of long OPE/OPV H-mer **36** by Sonogashira coupling.

3. Nomenclature of substituted H-mers

In the basic unsubstituted H-mer backbone, the central OPV segment joints two parallel OPE branches in a skewed manner that renders the molecule an italicized H-shape with a C_2 symmetry. Such an arrangement imparts the H-mer rather complex conjugation and cross-conjugation patterns. Of note is that the longest linear conjugation path in the H-mer consists of the OPV unit and two *ortho*-OPE segments (highlighted in pink color in the structures shown in Fig. 2). The unsubstituted H-mer is achiral itself; however,

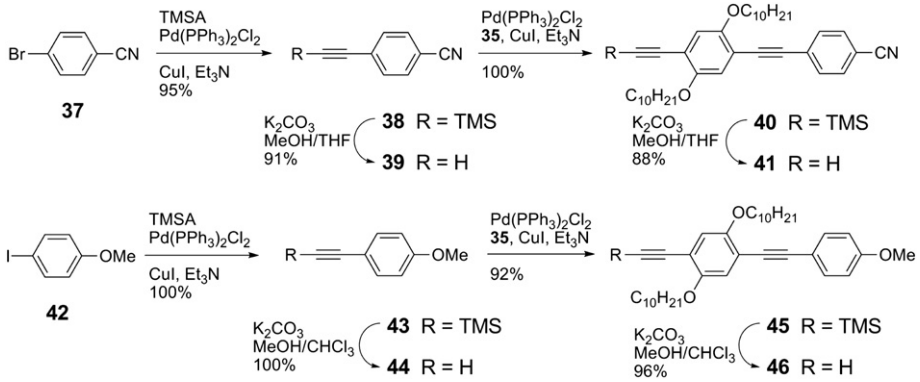

Scheme 7. Synthesis of D/A-substituted phenylacetylene dimers **41** and **46**.

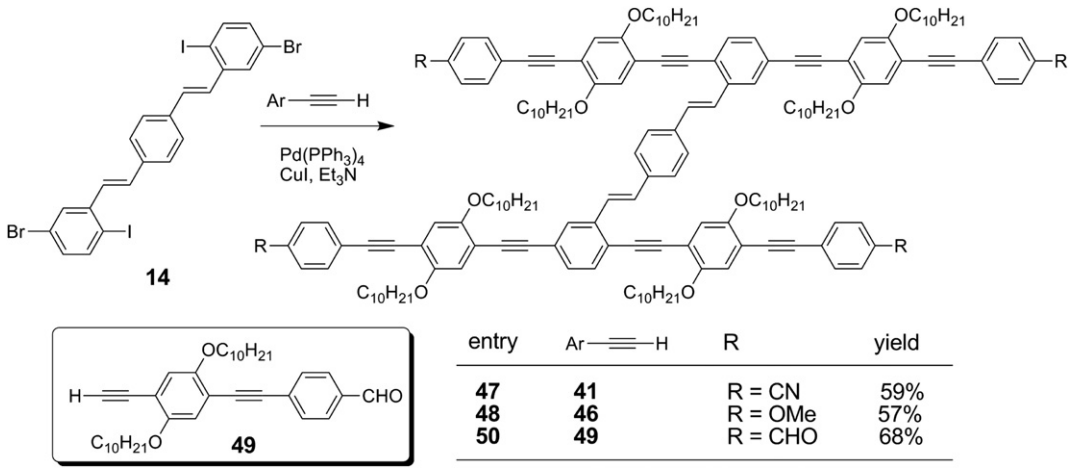

Scheme 8. Synthesis of D/A-substituted long OPE/OPV H-mers **47**, **48**, and **50** by Sonogashira coupling.

it provides a stereogenic element to give rise to stereoisomers in the cases that its termini are functionalized with different groups. To facility the following discussions on the structures and properties of diverse substituted H-mers, a simple naming rule is devised and illustrated in Fig. 2.

Depending on the length of the OPE branches, the H-mers are generally categorized as *SH* (short H-mers) and *LH* (long H-mers). The positions of terminal functionality attached to the H-mer backbone are designated by numbers shown in Fig. 2. In this way, the substituted H-mers can be unambiguously named. For example, short D/A substituted H-mer **29** is given a short name: *SH*-1,3-$(COOMe)_2$-2,4-$(NMe_2)_2$. Also, from a short name, the exact structure and substitution pattern of each H-mer derivative can be easily perceived. In particular, the structural differences between the two stereoisomers, **55** (*LH*-1,3-$(CN)_2$-2,4-$(OMe)_2$) and **56** (*LH*-2,4-$(CN)_2$-1,3-$(OMe)_2$), can be clearly noted from their short names. As the 1,3-terminal positions are in direct conjugation and the 2,4-terminal positions are in cross-conjugation, the electronic substitution effects experienced by the two isomers are in theory different; in compound **55**, the longest conjugation path is endcapped with electron-accepting CN groups, whereas in compound **56** the longest conjugation path is ended with electron-donating OMe groups.

4. Electronic substitution effects on the steady-state electronic spectroscopic properties of H-mers

The electronic properties of the H-mers in the ground and excited states have been investigated by UV–vis absorption and fluorescence spectroscopy. Detailed electronic spectra are given in Fig. 3 and spectroscopic data are summarized in Table 1.

All the compounds have similar patterns of electronic transitions; however, the band intensities vary as a function of the substituent pattern. These spectral features are clearly illustrated in Fig. 3A. The unsubstituted short H-mer **17** (*SH*) shows a broad unstructured $\pi \rightarrow \pi^*$ transition band with λ_{max} at 327 and 386 nm, along with a low-energy tail at ca. 410 nm. When the terminal positions of the short H-mer are substituted with D/A or D-A groups, the absorption spectral envelopes are red-shifted as a response to changes in the electronic wavefunctions, which arise from alterations of the orbital energies. D-substitution (in the case

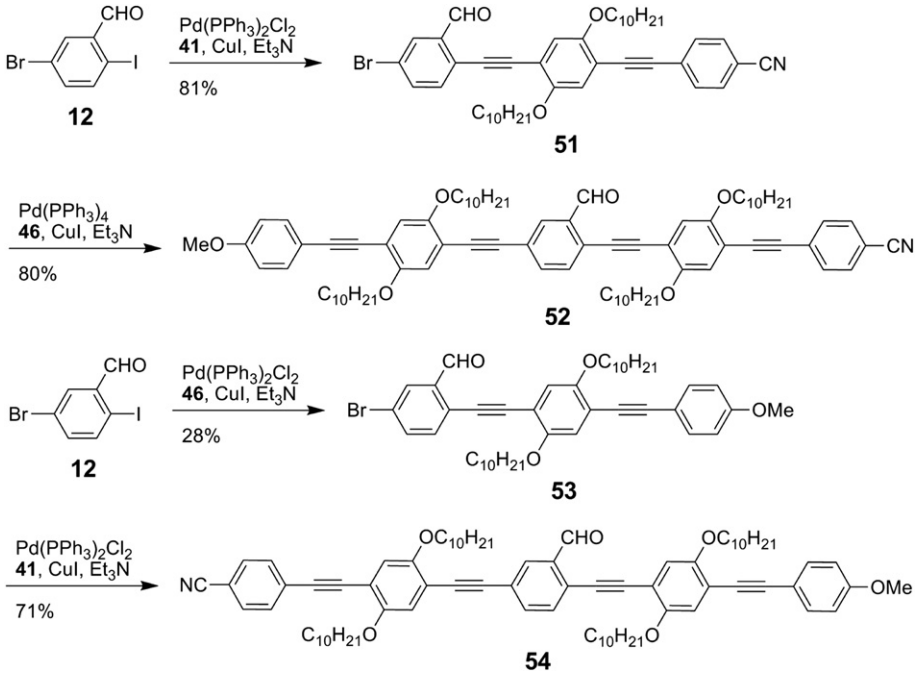

Scheme 9. Synthesis of D/A-substituted phenylacetylene pentamers **52** and **54** by Sonogashira coupling.

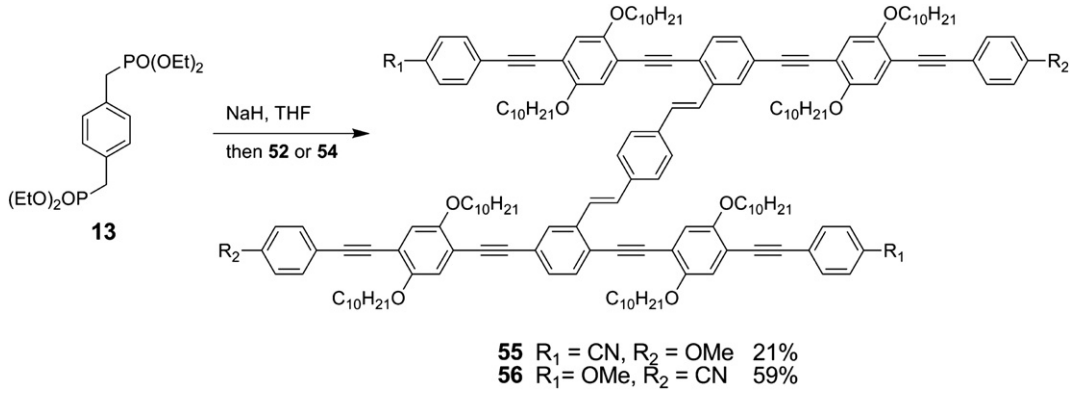

Scheme 10. Synthesis of D/A-substituted long OPE/OPV H-mers **55** and **56** by HWE reaction.

of **19**, *SH*-$(NMe_2)_4$) gives rise to the most notable red shift of the lowest-energy absorption band, while A-substitution (in the case of **18**, *SH*-$(COOMe)_4$) affords a very small red shift. When the terminal positions of the short H-mer backbone are functionalized with two donor and two acceptor groups (in the case of **29**, *SH*-1,3-$(COOMe)_2$-2,4-$(NMe_2)_2$), the small change in the energy of the maxima of the spectral envelope (λ_{max}) is likely due to offsetting electronic substituent effects as evidenced by the nearly superimposable 410 nm transition with that of the **19** (*SH*-$(NMe_2)_4$).

The emission spectra of short H-mers are shown in Fig. 3B. *SH* **17** shows distinct vibronic progression at 425, 450, and 480(sh) nm with a vibronic spacing of 1310 cm^{-1} consistent with a C=C accepting mode. The vibronic features are still retained in the case of acceptor substitution (**18**, *SH*-$(COOMe)_4$), whereas in the cases of D- and D-A substitution (**19** and **29**) the emission spectra show broad and featureless bands, which are significantly shifted to lower energy (longer wavelength). The energetic trends found in the absorption data mirror those observed in the emission spectra presumably due to the similar vibrational and solvent reorganization energetics for analogous H-mers as manifested by their relatively constant Stokes shifts (Table 1).

Long unsubstituted H-mer **36** (*LH*) shows two resolved absorption bands at 324 and 376 nm (Fig. 3C). Upon substitution with A (**47** *LH*-$(CN)_4$) or D (**47** *LH*-$(OMe)_4$) groups, only a very small red shift is observed. Unlike the short H-mer series, D- or A-substitution does not result in any transitions readily assigned to a charge transfer transition. In the context of the discussion below, charge transfer bands are those transitions where an electron has been removed from a donor group to an acceptor group. It is interesting to note that the spectral features of the two D-A substituted *LH* isomers **55** and **56** are different. Compound **55** (*LH*-1,3-$(CN)_2$-2,4-$(OMe)_2$) has two A groups terminated at the ends of the longest conjugation path. The constitutional isomer **56** (*LH*-2,4-$(CN)_2$-1,3-$(OMe)_2$) has two D groups attached to the termini of the longest conjugation path as well. UV–vis absorption bands of **55** and **56** appear at similar wavelengths without any significant shifts. However, their molar absorptivities are dramatically different; in the low-energy region, the extinction coefficients of **55** are approximately doubled as those of **56**. These observations suggest that the intensities are due to the statistical effects. In this interpretation the chromophores are electronically uncoupled and do not interact with each other. Therefore, the intensities of the

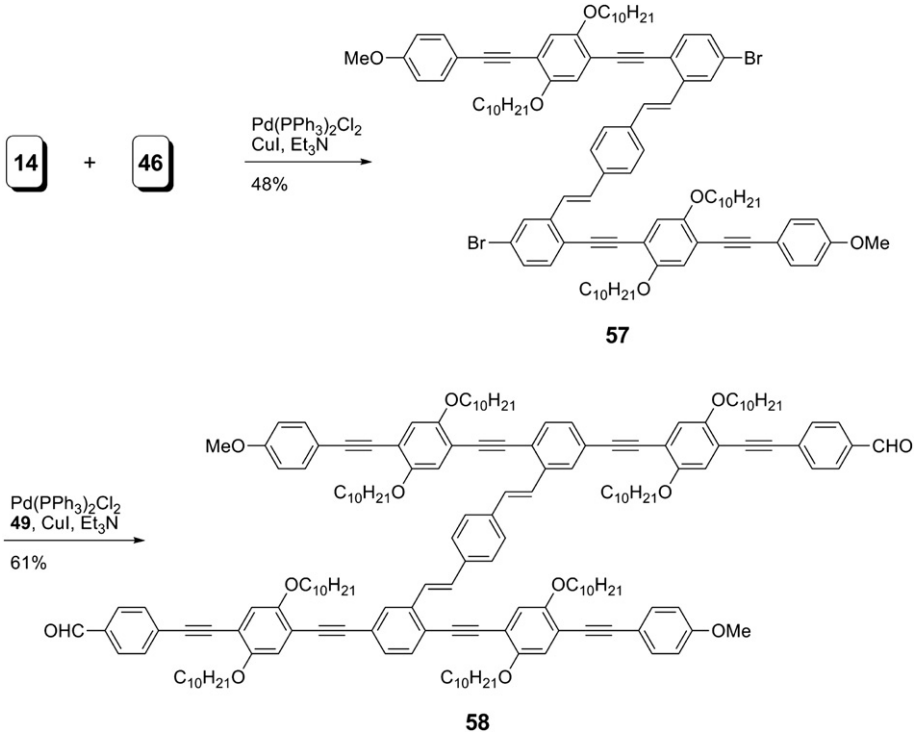

Scheme 11. Synthesis of D/A-substituted long OPE/OPV H-mer **58** by Sonogashira coupling.

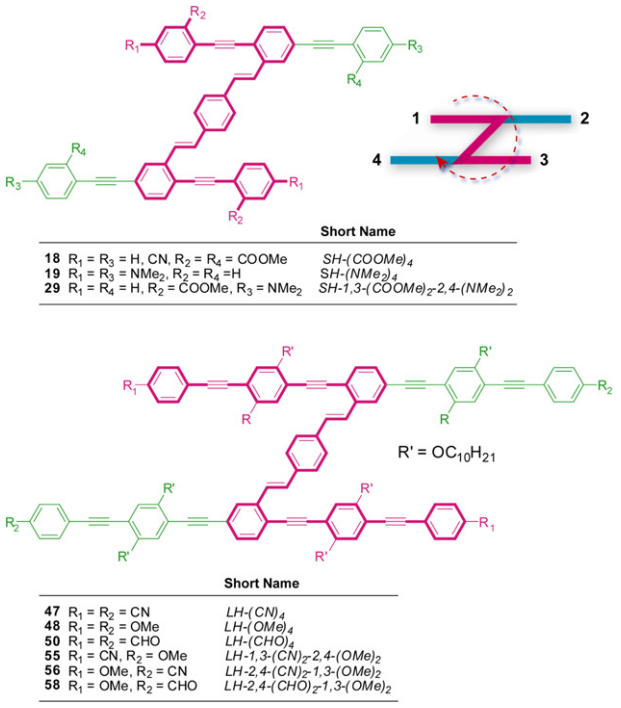

Fig. 2. Nomenclature of substituted H-mers.

transitions are linear combination of independent chromophores on the same molecules. These trends are clearly illustrated in Fig. 3C.

The fluorescence spectrum of *LH* **36** shows characteristic vibronic progression at 439 and 465 nm with a spacing (1275 cm^{-1}) similar to that of *SH* **17**. Upon D/A substitution, the emission bands show red shifts by 13–15 nm relative to **36** (Fig. 3D) with their lineshapes slightly broadened. In comparison with the short H-mers, electronic substitution effects on both the absorption and emission spectra of long H-mers are significantly reduced with the extension of the conjugation length of the OPE branch. Apparently, the effective conjugation paths have been attenuated due to the presence of multi-substituents on the long OPE branches. The 1,2- and 5,6-substituent patterns result in significant reduction of the electronic communication between the terminal electronic substituents attached to the long H-mer backbone. The mechanism for the interaction of the substituents through the long H-mer backbone appears to be subtle and awaits further investigations to clearly elucidate.

5. Spectroscopic responses of H-mers in binding with TFA and transition metal ions

The synthesized H-mers contain π-electron rich backbones and substituents, which may interact covalently with added acids or transition metal ions. Therefore, Lewis acid and base interactions between the added analytes and H-mers should lead to significant changes in conformation and electronic nature. In principle, the H-mer would display spectral responses to certain chemical species, which forms the basis for chemical sensors. The response of absorption/fluorescence provides a powerful and sensitive reporter for functional colorimetric molecular sensors. Described below are the results of experiments where analytes, such as metal ions and proton were added to H-mers to screen for potential highly selective chemosensors. A series of titrations were undertaken to explore the Lewis acid and base chemistry for H-mers with various chemicals, including a strong organic acid—trifluoroacetic acid (TFA), and five selected metal triflate salts—AgOTf, $Cu(OTf)_2$, $Zn(OTf)_2$, $Ba(OTf)_2$, and $Mg(OTf)_2$.

The addition of selected analytes to solutions of H-mers results in different absorption and emission spectral responses. Table 2 summarizes the spectroscopic properties of the H-mer adducts that are formed over the course of titrations. For the short H-mers, two oligomers **19** and **29** carrying NMe_2 as the end group show significant spectroscopic changes as a function of concentration of TFA and two transition metal ions Ag^+ and Cu^{2+} (Figs. 4 and 5, respectively).

The titration of H-mer **19** (*SH*-$(NMe_2)_4$) with TFA (Fig. 4A) results in attenuation of the low-energy absorption band at 367 nm, with concomitant growth of a new band at 329 nm. The spectral changes are associated with the protonation of the four NMe_2 groups by TFA, which alters the nature of the NMe_2 from electron-donating to

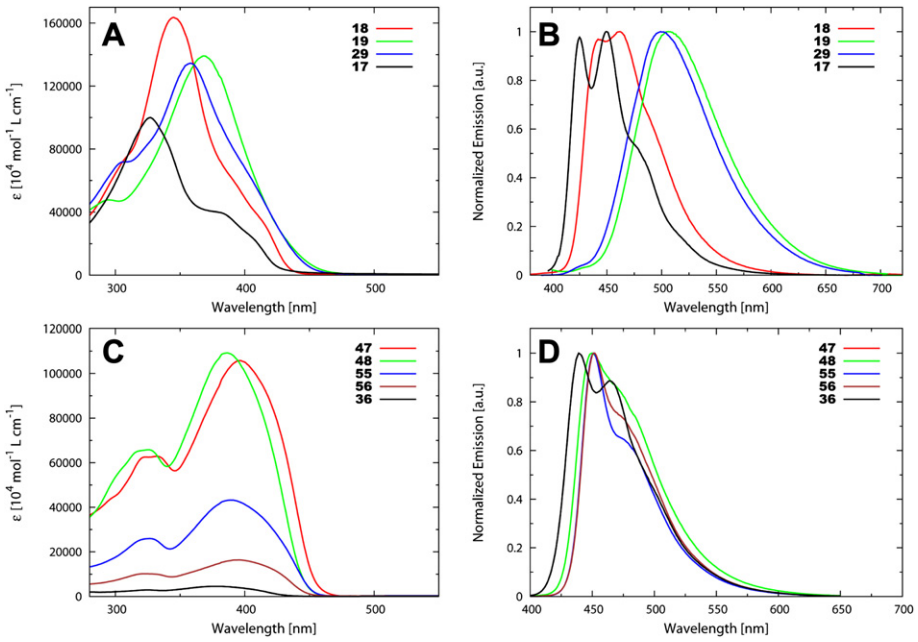

Fig. 3. (A) UV–vis spectra of short H-mers. (B) Fluorescence spectra of short H-mers. (C) UV–vis spectra of long H-mers. (D) Fluorescence spectra of long H-mers.

Table 1
Summary of photophysical data for H-mers measured in deoxygenated $CHCl_3$ at rt

Entry	Absorption		Emission			Stokes shift (cm^{-1})
	λ (nm)	ϵ (10^4 M^{-1} cm^{-1})	λ (nm)	Φ	τ (ns)	
17	327	9.9	425	0.49	1.2	2360
	386	3.8	450		1.2	
			480(sh)		1.3	6370
18	303(sh)	7.6	442	0.36		
	345	17	462		2.0	
	415(sh)	3.3				
19	295	0.48	506	0.43	6.4	7910
	367	1.4				
29	305(sh)	7.4	500	0.56	5.3	8330
	358	14				
36	324	0.29	439	0.54	2.0	3810
	376	0.46	465		2.2	
47	322	6.7	450	0.72	1.3	2990
	397	11	480(sh)		1.3	
48	325	6.5	450	0.52	1.6	3710
	368	11	479(sh)		1.8	
55	326	1.9	450	0.70	1.3	3380
	391	3.2	480(sh)		1.4	
56	323	1.0	451	0.62	1.5	3080
	393	1.6	488(sh)		1.6	

Table 2
Summary of sensing effectiveness of H-mers towards TFA various metal triflate salts

Entry	TFA	Ag^+	Cu^{2+}	Zn^{2+}	Ba^{2+}	Mg^{2+}
17	–	–	–	–	–	–
18	–	–	–	–	–	–
19	+	+	+		–	–
29	+	+	+	–	–	–
36	–	+	–	–	–	–
47	–	–	–	–	–	–
48	–	–	–	–	–	–
55	–	–	–	–	–	–
56	–	–	–	–	–	–

Note that '+' denotes significant absorption and fluorescence spectral changes observed in titration, '–' signifies no detectable spectral changes during titration.

electron-accepting $[NHMe_2]^+$. Overall, the absorption spectrum of **19** shows a dramatic blue shift in binding with TFA. The final spectrum after saturation with TFA is quantitatively similar to the absorption spectrum of unsubstituted short H-mer **17** (*SH*) as shown in Fig. 3A. The fluorescence spectrum of **19** also exhibits a similar blue shift with the increasing concentration of TFA (Fig. 4B). The low-energy emission at 506 nm is considerably attenuated, with appearance of a structured emission spectrum having bands at 431, 452, and 485 nm (sh). The spectral shape after complete protonation by TFA (ca. 12,000 M equiv) is very similar to the emission spectra of **17** (*SH*) and **18** (*SH*-$(COOMe)_4$).

Titration of **19** with Ag^+ gives rise to similar absorption and fluorescence spectral changes to those observed for the TFA titration (Fig. 3C and D). The end point of Ag^+ titration requires only 14 M equiv, significantly less than that observed for TFA titration (ca. 12,000 M equiv). The large difference in the equilibrium constants for Ag^+ versus TFA is consistent with the hard and soft acid/base (HSAB) theory, where the binding affinity between the NMe_2 group and the soft Lewis acid Ag^+ is expected to be much larger than that of protonation.

Upon titration of **19** with TFA and Ag^+ (Fig. 4A–D), the shift of isosbestic points is observed, suggesting the involvement of multi-step processes in the reaction mechanism. Based on the global spectral fitting analysis (Table 3), a two-step binding mechanism is

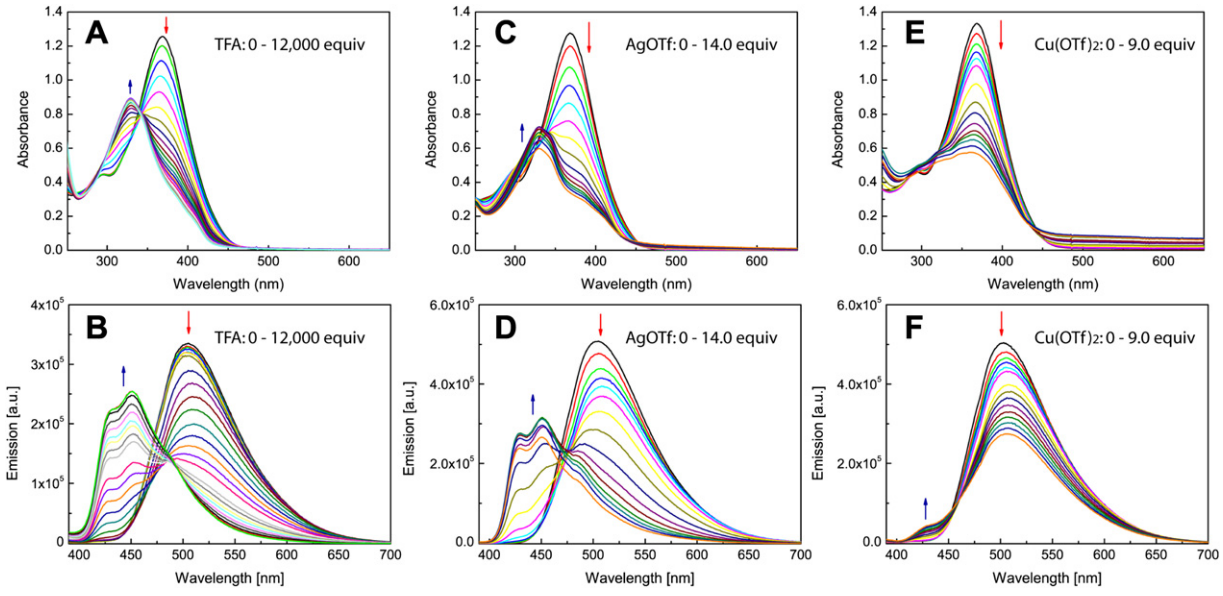

Fig. 4. UV–vis spectroscopic titrations of H-mer **19** (9.1 μM in $CHCl_3$) with (A) TFA, (C) AgOTf, and (E) $Cu(OTf)_2$. Fluorescence spectroscopic titrations of H-mer **19** (9.1 μM in $CHCl_3$) with (B) TFA, (D) AgOTf, and (F) $Cu(OTf)_2$.

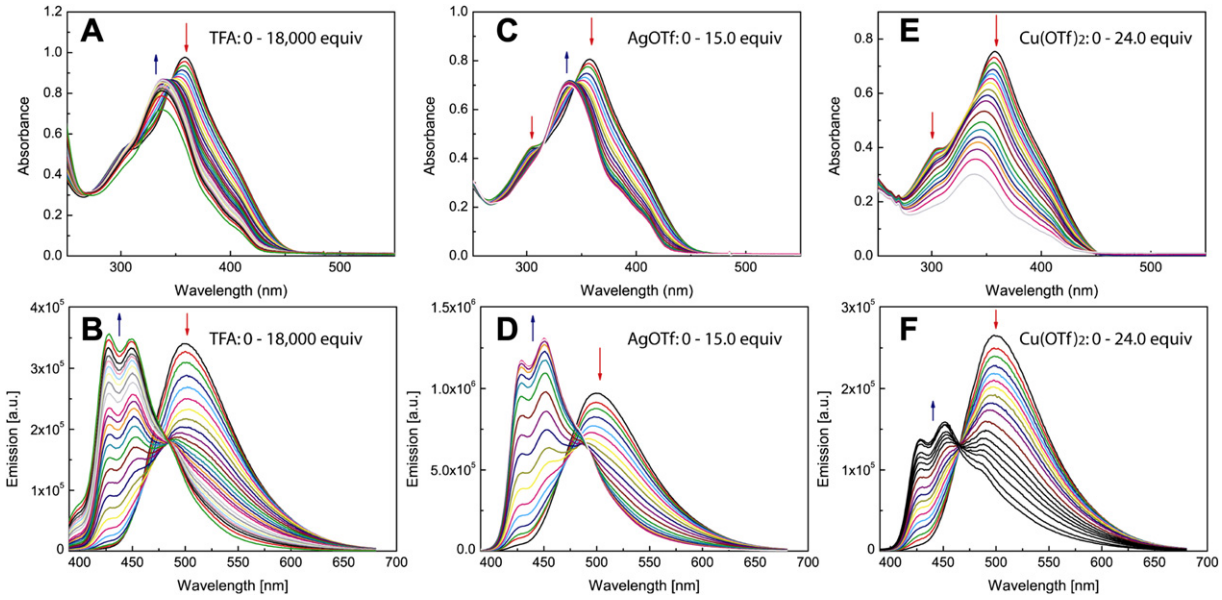

Fig. 5. UV–vis spectroscopic titrations of H-mer **29** (6.0 μM in $CHCl_3$) with (A) TFA, (C) AgOTf, and (E) $Cu(OTf)_2$. Fluorescence spectroscopic titrations of H-mer **29** (6.0 μM in $CHCl_3$) with (B) TFA (D) AgOTf, and (F) $Cu(OTf)_2$.

Table 3
Equilibrium constants for the binding of H-mers **19** and **29** to various chemical species in the ground and excited states

H-mer	Titrant	Ground state		Excited state	
		log K_1 (M^{-1})	log K_1K_2 (M^{-2})	log K_1 (M^{-1})	log K_1K_2 (M^{-2})
19	TFA	3.5±0.030	5.7±0.015	3.6±0.037	6.4±0.045
	AgOTf	9.6±0.28	18.8±0.28	10.6±0.53	19.4±0.50
	$Cu(OTf)_2$	10.4±0.030	22.2±0.29	13.4±0.74	22.8±0.74
29	TFA	3.4±0.063		2.7±0.058	
	AgOTf	9.1±0.046		8.8±0.088	
	$Cu(OTf)_2$	9.4±0.11		8.9±0.80	

proposed as illustrated in Scheme 12. The two NMe_2 groups located at the 1,3-positions are supposed to be protonated or coordinate with Ag^+ in the first step, while protonation or coordination at the 2,4-positions occurs in the second step (see Eq. 1 and 2, Scheme 12).

In comparison with TFA and Ag^+ titrations, the titration of **19** with Cu^{2+} yields a decrease of the intensity of ICT absorption band, but there is no shift for λ_{max} (Fig. 4E). Also, with the titration, the ICT band broadens resulting in a systematic increase in the UV–vis baseline and becomes more prominent as the saturation limit is reached. A similar effect is observed in the fluorescence spectra, whereas the emission peak at 506 nm is relatively unchanged (Fig. 4F). The absorption and emission behaviors suggest that the binding of Cu^{2+} to **19** has only a small perturbation on the electronic wavefunctions involved in the optical transitions.

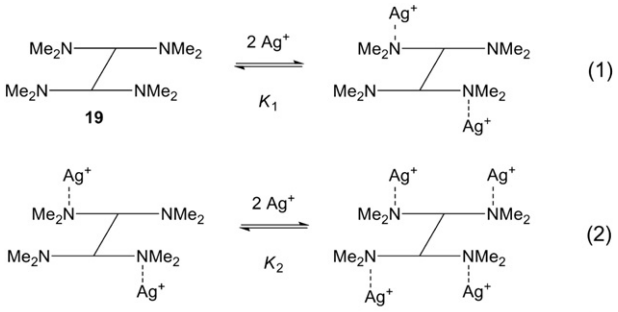

Scheme 12. Two-step mechanism for coordination of H-mer **19** with Ag^+.

Upon titration of D-A substituted short H-mer **29** (*SH*-1,3-$(COOMe)_2$-2,4-$(NMe_2)_2$) with TFA and Ag^+, the spectral changes are similar to the titration response of **19**. Global spectral fitting analysis reveals that the binding of **29** to TFA or Ag^+ involves only a one-step process (Table 3). The magnitude of binding constant K_1 is similar to that of NMe_2 substituted H-mer **19**, indicating that the binding constants are statistical and the two NMe_2 groups of **29** are independent and there is no long-range electronic communication between them. The COOMe groups do not participate in the binding reactions and act as spectator substituents. Unlike the case of D-substituted H-mer **19**, the titration of Cu^{2+} to D-A substituted H-mer **29** led to blue shift in the absorption spectrum (Fig. 5E). The fluorescence spectrum of **29** upon titration with Cu^{2+} is also blue-shifted with the appearance of structured emission profile. These results suggest that H-mer **29** binds to Cu^{2+} by a mechanism very different from that for H-mer **19**.

For the long H-mers, only the titration of **36** (*LH*) with Ag^+ shows significant absorption and emission changes. This is surprising given the relatively weak electronic substitution effect on the long H-mer backbone as described above. The UV–vis and fluorescence titration data for **36** with Ag^+ is given in Fig. 6.

As shown in Fig. 6A, the intensity of two absorption bands at 326 and 374 nm decrease with the increasing addition of Ag^+. Furthermore, there is an apparent increase of low-energy absorption tail ranging from 450 to 500 nm in the UV–vis absorption spectra. In the fluorescence spectra, titration of Ag^+ reduces the radiative quantum yield of the H-mer as a result of metal ion coordination (Fig. 6B). Although the observation of an isosbestic point

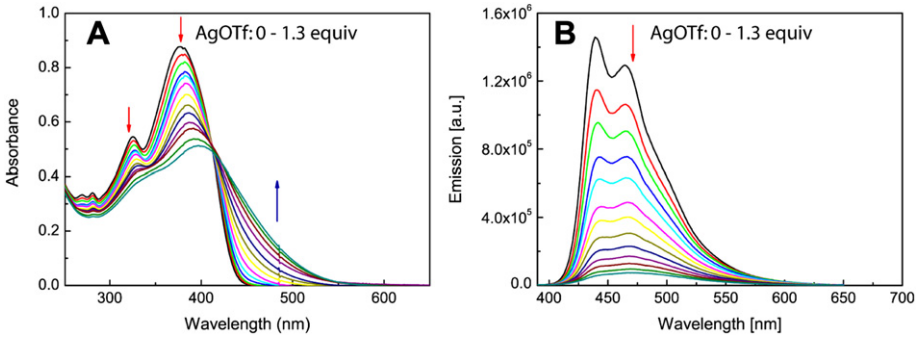

Fig. 6. (A) UV–vis and (B) fluorescence spectroscopic titrations of H-mer **36** (17 mM in $CHCl_3$) with AgOTf.

in the UV–vis titration curves suggests an equilibrium of two species, the exact reaction mechanism for **36** and Ag^+ has not been established yet. A hypothesis can be made on the assumption that the external alkynyl moieties in **36** interact with Ag^+ to form supramolecular aggregates in solution. Detailed NMR spectroscopic measurements are currently underway for further understanding.

6. Conclusions

In conclusion, this report delineates the first full account of a new type of monodisperse H-shaped OPE/OPV co-oligomers (H-mers) in terms of iterative synthesis, structure–property relationship, and chemical sensing behavior. Sonogashira coupling and HWE olefination reaction are two key steps in constructing the H-mer backbone. For the synthesis of short H-mers, a convergent strategy using Sonogashira coupling as the final step has been proven more effective than the one using the HWE reaction. For long H-mers, however, both synthetic strategies have been demonstrated successful in making the H-mer backbones. Electronic substitution effects have been investigated by UV–vis and fluorescence spectroscopy. Our results show that the short H-mer backbone is more susceptible to the electronic substituents attached to its termini, while the substitution effect and electronic communication in the long H-mer backbone are considerably attenuated as a result of its much longer π-conjugated paths. It is noteworthy that the OPE/OPV H-mer backbone serves an asymmetrical element to produce stereoisomers when its terminal positions are functionalized with different substituents. The electronic properties of such substituted H-mers are dependent on the exact substitution pattern. Short H-mers functionalized with amino groups can bind with TFA, Ag^+, and Cu^{2+} through acid–base interactions, resulting in pronounced spectral changes in UV–vis absorption and fluorescence spectra. The spectroscopic responses attest to the applicability of using H-mers as chromophores and fluorophores to construct functional chemosensors and biosensors.

7. Experimental section

7.1. General experimental

Chemicals and reagents were purchased from commercial suppliers in reagent grade and used without further purification. Solvents were dried prior to use: THF and CH_2Cl_2 were distilled from sodium/benzophenone ketyl; Et_3N and toluene were distilled from LiH. Palladium catalysts $Pd(PPh_3)_2Cl_2$ and $Pd(PPh_3)_4$ were prepared from $PdCl_2$ according to standard procedures. Precursors **8**–**13**,[62,85,88,89] **20** and **21**,[90,91] **35**,[81,83,85] **38** and **39**,[92] **43** and **44**[93] have been previously reported, and their synthetic procedures and characterizations are provided as Supplementary data. All reactions were performed in standard, dry glassware under an inert atmosphere of N_2 unless otherwise noted. Evaporations and concentrations were done at H_2O-aspirator pressure. Flash column chromatography was carried out with silica gel 60 (230–400 mesh). Thin-layer chromatography (TLC) was carried out with silica gel 60 F_{254} covered on plastic sheets and visualized by UV light or $KMnO_4$ stain.

Melting points (mp) were measured with a Fisher–Johns melting point apparatus and are uncorrected. ^1H and ^{13}C NMR spectra were measured on a Bruker Avance 500 MHz spectrometer. Chemical shifts (δ) are reported in parts per million down field from the signal of the internal reference $SiMe_4$. Coupling constants (J) are given in hertz. The coupling constants of some aryl proton signals are reported as pseudo first-order spin systems, even though they are second-order spin systems. Infrared spectra (IR) were recorded on a Bruker Tensor 27 spectrometer. UV–vis spectra were recorded on an Agilent 8453 UV–vis or a Cary 6000i UV–vis-NIR spectrophotometer. Fluorescence spectra were measured in deoxygenated $CHCl_3$ at ambient temperature using a Quantamaster 10,000 fluorimeter. Positive-mode high-resolution mass spectra (HRMS) were measured on a Waters GCT premier instrument equipped with a chemical ionization (CI) ion source and a QSTAR XL hybrid quadrupole/TOF mass spectrometer equipped with an *o*-MALDI ion source (Applied Biosystems). Binding constants (K) were determined by *SPECFIT* global analysis software package.[94]

7.2. Synthesis of 1,4-bis(5-bromo-2-iodostyryl)benzene (14)

To an oven-dried round-bottom flask protected under a N_2 atmosphere were charged compound **13** (472 mg, 1.25 mmol), NaH (75 mg, 3.1 mmol), and dry THF (10 mL). Upon gentle heating at 50 °C, the solution gradually turned into a light yellow color. Aldehyde **12** (775 mg, 2.49 mmol) dissolved in THF (5 mL) was added in small portions over a period of 1 h through a syringe. The reaction was kept under stirring and heating for another 2 h before workup. The small excess NaH was carefully quenched with HCl (aq 10%) and the mixture was extracted with $CHCl_3$ three times. The organic layer was washed with brine and dried over $MgSO_4$. Removal of $CHCl_3$ under vacuum resulted in a yellow solid, which was recrystallized from $CHCl_3$/MeOH (1:1, v/v) to give **14** (380 mg, 0.549 mmol, 45%) as a yellow solid. Mp 254–255 °C; IR (KBr) 3047, 1880, 1628, 1565, 1533 cm^{-1}; ^1H NMR ($CDCl_3$, 500 MHz) δ 7.76 (d, J=1.5 Hz, 2H), 7.72 (d, J=8.0 Hz, 2H), 7.58 (s, 4H), 7.26 (d, J=16.0 Hz, 2H), 7.10 (dd, J=8.5, 3.0 Hz, 2H), 6.98 (d, J=16.0 Hz, 2H). Meaningful ^{13}C NMR spectrum could not be obtained due to poor solubility. HRMS (CI) m/z calcd for $C_{22}H_{14}Br_2I_2$ 691.7531, found 692.7881 $[M+H]^+$.

7.3. Synthesis of OPV 15

To an oven-dried round-bottom flask protected under a N_2 atmosphere were charged compound **14** (171 mg, 0.247 mmol), trimethylsilylacetylene (0.30 g, 3.1 mmol), $PdCl_2(PPh_3)_2$ (25.5 mg,

0.0363 mmol), CuI (13.8 mg, 0.0726 mmol), and Et_3N (10 mL). The solution was bubbled by N_2 at rt for 5 min and then heated to 50 °C under stirring and N_2 protection overnight. After the reaction was completed as checked by TLC analysis, the solvent was removed by rotary evaporation. The resulting residue was diluted with $CHCl_3$. The mixture was filtered through a $MgSO_4$ pad. The solution obtained was sequentially washed with HCl (aq 10%) and brine. The organic layer was dried over $MgSO_4$ and concentrated under vacuum to give crude **15**, which was further purified by silica flash column chromatography (hexanes/CH_2Cl_2, 4:1) to yield compound **15** (135 mg, 0.202 mmol, 82%) as a yellow solid. Mp 262–263 °C; IR (KBr) 3031, 2959, 2898, 2155, 1633, 1478 cm^{-1}; ^1H NMR ($CDCl_3$, 500 MHz) δ 7.81 (br s, 2H), 7.68 (d, J=16.5 Hz, 2H), 7.57 (s, 4H,), 7.44 (d, J=8.5 Hz, 2H), 7.30 (dd, J=8.0, 1.5 Hz, 2H), 7.22 (d, J=16.0 Hz, 2H), 0.34 (s, 18H), 0.30 (s, 18H); ^{13}C NMR ($CDCl_3$, 125 MHz) δ 139.3, 137.2, 132.8, 130.6, 130.5, 128.2, 127.3, 126.3, 123.6, 122.3, 104.8, 103.3, 101.9, 96.4, 0.19, 0.15; HRMS (CI) m/z calcd for $C_{42}H_{50}Si_4$ 666.2990, found 667.3103 $[M+H]^+$.

7.4. Synthesis of OPV 16

To a solution of compound **15** (135 mg, 0.202 mmol) in MeOH/THF (1:1, 10 mL) was added K_2CO_3 (50 mg, 0.36 mmol). The mixture was stirred at rt for 1 h, then the solvent was removed by rotary evaporation. The residue was diluted in EtOAc and sequentially washed with HCl (aq 10%) and brine. The organic layer was dried over $MgSO_4$ and concentrated under vacuum to afford the crude product of **16**, which was further purified by silica flash column chromatography (hexanes/CH_2Cl_2, 4:1) to yield compound **16** (77 mg, 0.20 mmol, 100%) as a yellow solid. Mp >300 °C (dec); IR (KBr) 3275, 3030, 2155, 2099, 1635, 1538, 1478 cm^{-1}; ^1H NMR ($CDCl_3$, 500 MHz) δ 7.84 (d, J=1.5 Hz, 2H), 7.62 (d, J=16.5 Hz, 2H), 7.56 (s, 4H), 7.48 (d, J=8.5 Hz, 2H), 7.33 (dd, J=8.0, 2.5 Hz, 2H), 7.19 (d, J=16.5 Hz, 2H), 3.49 (s, 2H), 3.20 (s, 2H); ^{13}C NMR ($CDCl_3$, 125 MHz) δ 139.8, 137.3, 133.7, 131.4, 130.9, 128.7, 127.7, 126.0, 123.2, 121.9, 84.3, 83.5, 82.0, 79.3; HRMS (CI) m/z calcd for $C_{30}H_{18}$ 378.1409, found 379.1453 $[M+H]^+$

7.5. Synthesis of short H-mer 17 (*SH*)

To an oven-dried round-bottom flask protected under a N_2 atmosphere were charged compound **16** (30 mg, 0.079 mmol), iodobenzene (129 mg, 0.635 mmol), $PdCl_2(PPh_3)_2$ (11.2 mg, 0.0159 mmol), CuI (6.0 mg, 0.032 mmol), and piperidine (3 mL). The solution was degassed by bubbling with N_2 at rt for 5 min and then heated to 50 °C under stirring and N_2 protection overnight. After the reaction was completed as checked by TLC analysis, the solvent was removed by rotary evaporation. The resulting residue was diluted with $CHCl_3$. The mixture was filtered through a $MgSO_4$ pad. The solution obtained was sequentially washed with HCl (aq 10%) and brine. The organic layer was dried over $MgSO_4$ and concentrated under vacuum to give crude **17**, which was further purified by recrystallization from $CHCl_3$/hexanes to yield H-mer **17** (36 mg, 0.053 mmol, 67%) as a yellow solid. Mp >300 °C (dec); IR (KBr) 3262, 3052, 2208, 1631, 1597, 1499 cm^{-1}; ^1H NMR ($CDCl_3$, 500 MHz) δ 7.91 (br s, 2H), 7.73 (d, J=17.0 Hz, 2H), 7.61 (s, 4H), 7.60–7.57 (m, 8H), 7.55 (d, J=8.5 Hz, 2H), 7.41–7.37 (m, 14H), 7.28 (d, J=14.5 Hz, 2H). Meaningful ^{13}C NMR could not be obtained due to poor solubility; HRMS (MALDI-TOF) m/z calcd for $C_{54}H_{34}$ 682.2661, found 683.2675 $[M]^+$.

7.6. Synthesis of A-substituted short H-mer 18 (*SH*-(COOMe)$_4$)

To an oven-dried round-bottom flask protected under a N_2 atmosphere were charged compound **16** (26 mg, 0.069 mmol), methyl 2-iodobenzoate (108 mg, 0.412 mmol), $PdCl_2(PPh_3)_2$ (9.69 mg, 0.0138 mmol), CuI (5.24 mg, 0.0276 mmol), and Et_3N (3 mL). The solution was degassed by bubbling N_2 at rt for 5 min and then stirred at rt under N_2 protection for 18 h. After the reaction was completed as checked by TLC analysis, the solvent was removed by rotary evaporation. The resulting residue was diluted with $CHCl_3$. The mixture was filtered through a $MgSO_4$ pad. The solution obtained was sequentially washed with HCl (aq 10%) and brine. The organic layer was dried over $MgSO_4$ and concentrated under vacuum to give crude **18**, which was further purified by recrystallization from CH_2Cl_2/hexanes to yield compound **18** (44 mg, 0.048 mmol, 70%) as a yellow solid. Mp 175–176 °C; IR (KBr) 3060, 2948, 2840, 2208, 1728, 1595, 1532 cm^{-1}; ^1H NMR ($CDCl_3$, 500 MHz) δ 8.06–7.96 (m, 8H), 7.75 (s, 4H), 7.74–7.70 (m, 4H), 7.61 (d, J=8.5 Hz, 2H), 7.57–7.53 (m, 4H), 7.47–7.42 (m, 6H), 7.31 (d, J=16.5 Hz, 2H); ^{13}C NMR ($CDCl_3$, 125 MHz) δ 166.8, 166.5, 139.7, 137.3, 134.5, 134.4, 133.3, 132.10, 132.07, 132.0, 131.5, 131.2, 130.8, 130.4, 128.4, 128.3, 128.0, 127.8, 126.4, 124.2, 123.9, 123.8, 122.6, 95.0, 94.4, 93.3, 90.2, 52.49, 52.47 (one coincidental aromatic carbon not observed); HRMS (MALDI-TOF) m/z calcd for $C_{62}H_{42}O_8$ 914.2880, found 915.3173 $[M+H]^+$.

7.7. Synthesis of D-substituted short H-mer 19 (*SH*-(NMe$_2$)$_4$)

To an oven-dried round-bottom flask protected under a N_2 atmosphere were charged compound **16** (25 mg, 0.066 mmol), 4-iodo-*N*,*N*-dimethylaniline (140 mg, 0.568 mmol), $PdCl_2(PPh_3)_2$ (9.27 mg, 0.0132 mmol), CuI (5.0 mg, 0.026 mmol), and piperidine (3 mL). The solution was degassed by bubbling with N_2 at rt for 5 min and then stirred at rt under N_2 protection for 24 h. After the reaction was completed as checked by TLC analysis, the solvent was removed by rotary evaporation. The resulting residue was diluted with $CHCl_3$. The mixture was filtered through a $MgSO_4$ pad. The solution obtained was sequentially washed with HCl (aq 10%) and brine. The organic layer was dried over $MgSO_4$ and concentrated under vacuum to give crude **19**, which was further purified by recrystallization from $CHCl_3$/hexanes to yield compound **19** (44 mg, 0.052 mmol, 79%) as a yellow solid. Mp >300 °C (dec); IR (KBr) 3034, 2891, 2856, 2798, 2202, 1607, 1523, 1443 cm^{-1}; ^1H NMR ($CDCl_3$, 500 MHz) δ 7.84 (br s, 2H), 7.75 (d, J=16.0 Hz, 2H), 7.60 (s, 4H), 7.48–7.43 (m, 10H), 7.34 (d, J=8.0 Hz, 2H), 7.26 (d, J=16.5 Hz, 2H), 6.70–6.67 (m, 8H), 3.10 (s, 12H), 2.99 (s, 12H). Meaningful ^{13}C NMR spectrum could not be obtained due to poor solubility; HRMS (MALDI-TOF) m/z calcd for $C_{62}H_{54}N_4$ 854.4348, found 855.5049 $[M+H]^+$.

7.8. Synthesis of OPE 22

Compound **21** (80 mg, 0.52 mmol), methyl 2-iodobenzoate (273 mg, 1.04 mmol), $PdCl_2(PPh_3)_2$ (36 mg, 0.052 mmol), and CuI (20 mg, 0.104 mmol) were added to Et_3N (10 mL). The solution was bubbled by N_2 at rt for 5 min and then stirred for 3 h at rt. After the reaction was completed as checked by TLC analysis, the solvent was removed by rotary evaporation. The resulting residue was diluted with $CHCl_3$. The mixture was filtered through a $MgSO_4$ pad. The solution obtained was sequentially washed with HCl (aq 10%) and brine. The organic layer was dried over $MgSO_4$ and concentrated under vacuum to give crude **22**, which was further purified by silica flash column chromatography (hexanes/CH_2Cl_2, 1:1) to yield compound **22** (139 mg, 0.329 mmol, 63%) as a yellow solid. Mp 144–145 °C; IR (KBr) 2999, 2950, 2215, 1719, 1687, 1597, 1564, 1500, 1446 cm^{-1}; ^1H NMR ($CDCl_3$, 500 MHz) δ 10.74 (s, 1H), 8.14 (s, 1H) 8.04 (d, J=8.5 Hz, 1H), 8.01 (d, J=8.0 Hz, 1H), 7.77 (d, J=7.0 Hz, 1H), 7.71–7.69 (m, 2H), 7.66 (d, J=8.0, 1H), 7.57–7.51 (m, 2H), 7.47–7.41 (m, 2H), 3.99 (s, 3H), 3.97 (s, 3H); ^{13}C NMR ($CDCl_3$, 125 MHz) δ 191.8, 166.5, 166.2, 136.41, 136.39, 134.4, 134.3, 133.6, 132.08, 132.04, 131.95, 131.82, 130.9, 130.7, 130.4, 129.0, 128.6, 126.5, 124.4, 123.2,

122.9, 96.7, 92.9, 91.5, 89.9, 52.5, 52.4; HRMS (CI) *m*/*z* calcd for $C_{27}H_{18}O_5$ 422.1154, found 423.1265 $[M+H]^+$.

7.9. Synthesis of 5-bromo-2-((triisopropylsilyl)ethynyl) benzaldehyde (23)

Compound **12** (1.62 g, 5.20 mmol), triisopropylsilylacetylene (1.15 mL, 0.950 g, 5.20 mmol), $PdCl_2(PPh_3)_2$ (46 mg, 0.065 mmol), and CuI (25 mg, 0.13 mmol) were added to Et_3N (20 mL). The solution was bubbled with N_2 at rt for 5 min and then stirred at rt and under N_2 protection for 24 h. After the reaction was completed as checked by TLC analysis, the solvent was removed by rotary evaporation. The resulting residue was diluted with $CHCl_3$. The mixture was filtered through a $MgSO_4$ pad. The solution obtained was sequentially washed with HCl (aq 10%) and brine. The organic layer was dried over $MgSO_4$ and concentrated under vacuum to give crude **23**, which was further purified by silica flash column chromatography (hexanes/CH_2Cl_2, 4:1) to yield compound **23** (1.78 g, 4.87 mmol, 94%) as a colorless oil. IR (KBr) 2944, 2891, 2866, 2736, 2156, 1695, 1582, 1469, 1383 cm^{-1}; ^1H NMR ($CDCl_3$, 500 MHz) δ 10.53 (s, 1H), 8.05 (d, *J*=2.0 Hz, 1H), 7.67 (dd, *J*=8.5, 1.5 Hz, 1H), 7.47 (d, *J*=8.0 Hz, 1H), 1.15 (s, 21H); ^{13}C NMR ($CDCl_3$, 125 MHz) δ 190.4, 137.5, 136.7, 135.4, 130.1, 125.9, 123.4, 101.1, 100.9, 18.8, 11.4; HRMS (CI) *m*/*z* calcd for $C_{18}H_{25}BrOSi$ 364.0858, found 365.1071 $[M+H]^+$.

7.10. Synthesis of 2-((triisopropylsilyl)ethynyl)-5-((trimethylsilyl)ethynyl)benzaldehyde (24)

Compound **23** (417 mg, 1.14 mmol), trimethylsilylacetylene (0.322 mL, 2.28 mmol, mmol), $PdCl_2(PPh_3)_2$ (20 mg, 0.029 mmol), and CuI (11 mg, 0.057 mmol) were added to Et_3N (10 mL). The solution was bubbled with N_2 at rt for 5 min and then stirred at 60 °C under N_2 protection for 12 h. After the reaction was completed as checked by TLC analysis, the solvent was removed by rotary evaporation. The resulting residue was diluted with $CHCl_3$. The mixture was filtered through a $MgSO_4$ pad. The solution obtained was sequentially washed with HCl (aq 10%) and brine. The organic layer was dried over $MgSO_4$ and concentrated under vacuum to give crude **24**, which was further purified by silica flash column chromatography (hexanes/CH_2Cl_2, 17:1) to yield compound **24** (431 mg, 1.13 mmol, 99%) as a colorless oil. ^1H NMR ($CDCl_3$, 500 MHz) δ 10.58 (s, 1H), 8.01 (d, *J*=1.5 Hz, 1H), 7.61 (dd, *J*=8.0, 1.5 Hz, 1H), 7.54 (d, *J*=8.0 Hz, 1H), 1.16 (s, 21H), 0.28 (s, 9H); ^{13}C NMR ($CDCl_3$, 125 MHz) δ 190.9, 136.5, 136.3, 133.9, 130.7, 126.6, 124.1, 103.4, 101.9, 101.3, 98.0, 18.8, 11.4, 0.0; HRMS (CI) *m*/*z* calcd for $C_{23}H_{34}OSi_2$ 382.2148, found 383.2285 $[M+H]^+$.

7.11. Synthesis of 5-ethynyl-2-((triisopropylsilyl)ethynyl) benzaldehyde (25)

To a solution of compound **24** (431 mg, 1.13 mmol) in MeOH/THF (12 mL, 1:1) was added K_2CO_3 (50 mg, 0.36 mmol). The mixture was stirred at rt for 1 h, then the solvent was removed by rotary evaporation. The residue was diluted in CH_2Cl_2 and sequentially washed with HCl (aq 10%) and brine. The organic layer was dried over $MgSO_4$ and concentrated under vacuum to afford crude **25**, which was further purified by silica flash column chromatography (hexanes/CH_2Cl_2, 4:1) to yield compound **25** (371 mg, 1.2 mmol, 100%) as a colorless oil. ^1H NMR ($CDCl_3$, 500 MHz) δ 10.57 (s, 1H), 8.02 (d, *J*=2.0 Hz, 1H), 7.63 (dd, *J*=7.5, 2.0 Hz, 1H), 7.55 (d, *J*=7.5 Hz, 1H), 3.23 (s, 1H), 1.15 (s, 21H); ^{13}C NMR ($CDCl_3$, 125 MHz) δ 190.8, 136.8, 136.3, 134.0, 130.8, 127.1, 123.0, 101.69, 101.63, 82.2, 80.3, 18.8, 11.4; HRMS (CI) *m*/*z* calcd for $C_{20}H_{26}OSi$ 310.1753, found 311.1815 $[M+H]^+$.

7.12. Synthesis of methyl 2-((3-formyl-4-((triisopropylsilyl) ethynyl)phenyl)ethynyl)benzoate (26)

Compound **25** (181 mg, 0.583 mmol), methyl 2-iodobenzoate (153 mg, 0.583 mmol), $PdCl_2(PPh_3)_2$ (21 mg, 0.0293 mmol), and CuI (11.1 mg, 0.0586 mmol) were added to Et_3N (8 mL). The solution was bubbled with N_2 at rt for 5 min and then stirred at rt and under N_2 protection for 5 h. After the reaction was completed as checked by TLC analysis, the solvent was removed by rotary evaporation. The resulting residue was diluted with $CHCl_3$. The mixture was filtered through a $MgSO_4$ pad. The solution obtained was sequentially washed with aq HCl (10%) and brine. The organic layer was dried over $MgSO_4$ and concentrated under vacuum to give crude **26**, which was further purified by silica flash column chromatography (hexanes/CH_2Cl_2, 3:2) to yield compound **26** (196 mg, 0.441 mmol, 76%) as a white solid. Mp 82–83 °C; IR (KBr) 2942, 2890, 2865, 2153, 1710, 1694, 1600, 1493, 1463, 1450, 1384 cm^{-1}; ^1H NMR ($CDCl_3$, 500 MHz) δ 10.60 (s, 1H), 8.09 (d, *J*=1.0 Hz, 1H), 7.99 (d, *J*=8.5 Hz, 1H), 7.72 (dd, *J*=8.5, 1.0 Hz, 1H), 7.64 (d, *J*=8.0 Hz, 1H), 7.58 (d, *J*=8.5 Hz, 1H), 7.51 (t, *J*=8.5 Hz, 1H), 7.41 (t, *J*=8.0 Hz, 1H), 3.97 (s, 3H), 1.16 (s, 21H); ^{13}C NMR ($CDCl_3$, 125 MHz) δ 191.0, 166.5, 136.38, 136.35, 134.3, 134.0, 132.1, 132.0, 130.8, 130.3, 128.6, 126.6, 124.3, 123.2, 102.0, 101.4, 92.8, 91.4, 52.4, 18.8, 11.4; HRMS (CI) *m*/*z* calcd for $C_{28}H_{32}O_4Si$ 444.2121, found 445.2143 $[M+H]^+$.

7.13. Synthesis of methyl 2-((4-ethynyl-3-formylphenyl) ethynyl)benzoate (27)

To a solution of compound **26** (195 mg, 0.439 mmol) in THF (8 mL) was added TBAF (0.05 mL, 1 M in THF, 0.05 mmol). The mixture was stirred at rt for 10 min, and the solvent was removed by rotary evaporation. The residue was dissolved in $CHCl_3$ and sequentially washed with HCl (aq 10%) and brine. The organic layer dried over $MgSO_4$. Filtration to remove $MgSO_4$ followed by evaporation under vacuum afforded the crude product, which was purified by silica flash column chromatography (hexanes/CH_2Cl_2, 7:3) to yield compound **27** as a yellow solid (99 mg, 0.34 mmol, 78%). Mp 120–121 °C; IR (KBr) 3251, 2960, 2855, 2152, 2101, 1724, 1692, 1600, 1566, 1492, 1433, 1389 cm^{-1}; ^1H NMR ($CDCl_3$, 500 MHz) δ 10.52 (s, 1H), 8.10 (d, *J*=1.5 Hz, 1H), 8.01 (d, *J*=8.0 Hz, 1H), 7.75 (dd, *J*=8.0, 1.5 Hz, 1H), 7.66 (d, *J*=8.0 Hz, 1H), 7.61 (d, *J*=8.5 Hz, 1H), 7.53 (t, *J*=8.5 Hz, 1H), 7.43 (t, *J*=8.0 Hz, 1H), 3.98 (s, 3H), 3.58 (s, 1H); ^{13}C NMR ($CDCl_3$, 125 MHz) δ 190.8, 166.5, 136.7, 136.5, 134.4, 134.1, 132.2, 132.0, 130.8, 130.7, 128.7, 125.0, 124.9, 123.1, 92.6, 91.6, 86.0, 79.3, 52.5; HRMS (CI) *m*/*z* calcd for $C_{19}H_{12}O_3$ 288.0786, found 289.0852 $[M+H]^+$.

7.14. Synthesis of OPE 28

Compound **27** (99 mg, 0.34 mmol), 4-iodo-*N*,*N*-dimethylaniline (85 mg, 0.34 mmol), $PdCl_2(PPh_3)_2$ (12 mg, 0.017 mmol), and CuI (6.5 mg, 0.034 mmol) were added to Et_3N (6 mL). The solution was bubbled with N_2 at rt for 5 min and then stirred at 40 °C under N_2 protection for 7 h. After the reaction was completed as checked by TLC analysis, the solvent was removed by rotary evaporation. The resulting residue was diluted with $CHCl_3$. The mixture was filtered through a $MgSO_4$ pad. The solution obtained was sequentially washed with HCl (aq 10%) and brine. The organic layer was dried over $MgSO_4$ and concentrated under vacuum to give crude **28**, which was further purified by silica flash column chromatography (hexanes/CH_2Cl_2, 1:1) to yield compound **28** (65 mg, 0.16 mmol, 47%) as a white solid. Mp 151–152 °C; IR (KBr) 2925, 2198, 1730, 1688, 1610, 1526, 1492, 1446, 1432, 1384 cm^{-1}; ^1H NMR ($CDCl_3$, 500 MHz) δ 10.64 (s, 1H), 8.10 (d, *J*=1.0 Hz, 1H), 8.01 (d, *J*=8.0 Hz, 1H), 7.72 (dd, *J*=8.5, 1.0 Hz, 1H), 7.66 (d, *J*=8.5 Hz, 1H), 7.58 (d, *J*=8.5 Hz, 1H), 7.52 (t, *J*=8.5 Hz, 1H), 7.45 (d, *J*=9.0 Hz, 1H), 7.42 (t,

J=8.0 Hz, 1H), 6.68 (d, J=9.0 Hz, 1H), 3.99 (s, 3H), 3.02 (s, 6H); ^{13}C NMR ($CDCl_3$, 125 MHz) δ 191.5, 166.6, 150.9, 136.5, 135.4, 134.3, 133.2, 132.9, 132.1, 132.0, 130.8, 130.7, 128.5, 127.9, 123.4, 123.0, 111.9, 108.7, 100.6, 93.2, 90.9, 83.7, 52.5, 40.3; HRMS (CI) m/z calcd for $C_{27}H_{21}NO_3$ 407.1521, found 408.1653 $[M+H]^+$.

7.15. Synthesis of OPV 30

To an oven-dried round-bottom flask protected under a N_2 atmosphere were charged compound **13** (51.8 mg, 0.137 mmol), NaH (9.9 mg, 0.41 mmol), and dry THF (4 mL). Upon gentle heating at 40 °C, the solution gradually turned into a light yellow color. Aldehyde **23** (100 mg, 0.274 mmol) dissolved in THF (4 mL) was added in small portions over a period of 1 h through a syringe. The reaction was kept under stirring and heating for another 0.5 h before workup. The small excess NaH was carefully quenched with HCl (aq 10%) and the mixture was extracted with $CHCl_3$ three times. The organic layer was dried over $MgSO_4$ and concentrated under vacuum to give crude **30**, which was further purified by silica flash column chromatography (hexanes/CH_2Cl_2, 9:1) to yield compound **30** (50 mg, 0.062 mmol, 45%) as a yellow solid. Mp 174–175 °C; IR (KBr) 2941, 2890, 2864, 2152, 1631, 1579, 1560, 1541, 1510, 1467 cm^{-1}; ^{1}H NMR ($CDCl_3$, 500 MHz) δ 7.83 (d, J=1.5 Hz, 2H), 7.67 (d, J=16.0 Hz, 2H), 7.52 (s, 4H), 7.36 (d, J=8.5 Hz, 2H), 7.31 (dd, J=7.5, 1.5 Hz, 2H), 7.14 (d, J=16.5 Hz, 2H), 1.18 (s, 42H); ^{13}C NMR ($CDCl_3$, 125 MHz) δ 141.0, 137.0, 134.7, 131.0, 130.3, 127.53, 127.46, 125.8, 123.1, 121.6, 104.6, 97.6, 19.0, 11.6; HRMS (CI) m/z calcd for $C_{44}H_{56}Br_2Si_2$ 800.2267, found 801.2343 $[M+H]^+$.

7.16. Synthesis of OPV 31

Compound **30** (305 mg, 0.381 mmol), trimethylsilylacetylene (0.14 g, 1.4 mmol), $PdCl_2(PPh_3)_2$ (26.8 mg, 0.0381 mmol), and CuI (14.5 mg, 0.0762 mmol) were added to Et_3N (10 mL). The solution was bubbled with N_2 at rt for 5 min and then stirred at 60 °C under N_2 protection for 12 h. After the reaction was completed as checked by TLC analysis, the solvent was removed by rotary evaporation. The resulting residue was diluted with $CHCl_3$. The mixture was filtered through a $MgSO_4$ pad. The solution obtained was sequentially washed with HCl (aq 10%) and brine. The organic layer was dried over $MgSO_4$ and concentrated under vacuum to give crude **31**, which was further purified by silica flash column chromatography (hexanes/CH_2Cl_2, 19:1) to yield compound **31** (297 mg, 0.356 mmol, 93%) as a yellow solid. Mp 211–212 °C; IR (KBr) 2943, 2893, 2865, 2154, 1632, 1595, 1534, 1511, 1477 cm^{-1}; ^{1}H NMR ($CDCl_3$, 500 MHz) δ 7.82 (br s, 2H), 7.71 (d, J=16.5 Hz, 2H), 7.53 (s, 4H), 7.44 (d, J=7.0 Hz, 2H) 7.28 (dd, J=8.0, 1.0 Hz, 2H), 7.19 (d, J=16.5 Hz, 2H), 1.19 (s, 42H), 0.29 (s, 18H); ^{13}C NMR ($CDCl_3$, 125 MHz) δ 139.2, 137.1, 133.3, 130.6, 130.5, 128.1, 127.7, 126.2, 123.5, 122.7, 105.2, 104.9, 98.2, 96.2, 19.0, 11.6, 0.14; HRMS (CI) m/z calcd $C_{54}H_{74}Si_4$ 834.4868, found 835.5097 $[M+H]^+$.

7.17. Synthesis of OPV 32

To a solution of compound **31** (335 mg, 0.401 mmol) in MeOH/THF (12 mL, 1:1) was added K_2CO_3 (50 mg, 0.36 mmol). The mixture was stirred at rt for 15 min, then the solvent was removed by rotary evaporation. The residue was diluted with EtOAc and sequentially washed with HCl (aq 10%) and brine. The organic layer was dried over $MgSO_4$ and concentrated under vacuum to afford crude **32**, which was further purified by silica flash column chromatography (hexanes/CH_2Cl_2, 19:1) to yield compound **32** (220 mg, 0.318 mmol, 79%) as a yellow solid. Mp 143–144 °C; IR (KBr) 3300, 3033, 2942, 2891, 2864, 2149, 1632, 1596, 1536, 1511, 1464 cm^{-1}; ^{1}H NMR ($CDCl_3$, 500 MHz) δ 7.87 (d, J=1.0 Hz, 2H), 7.74 (d, J=16.0 Hz, 2H), 7.55 (s, 4H), 7.34 (dd, J=8.5, 1.0 Hz, 2H), 7.21 (d, J=16.5 Hz, 2H), 3.21 (s, 2H), 1.22 (s, 42H); ^{13}C NMR ($CDCl_3$, 125 MHz) δ 139.3, 137.1, 133.4, 130.7, 130.6, 128.3, 127.4, 126.1, 123.1, 122.4, 105.0, 98.4, 83.5, 78.9, 19.0, 11.6; HRMS (CI) m/z calcd for $C_{48}H_{58}Si_2$ 690.4077, found 691.4300 $[M+H]^+$.

7.18. Synthesis of OPE/OPV 33

To an oven-dried round-bottom flask protected under a N_2 atmosphere were charged compound **32** (220 mg, 0.318 mmol), methyl 2-iodobenzoate (168 mg, 0.637 mmol), $PdCl_2(PPh_3)_2$ (22 mg, 0.032 mmol), CuI (12 mg, 0.064 mmol), and Et_3N (10 mL). The solution was bubbled with N_2 at rt for 5 min and then stirred at 40 °C under N_2 protection for 12 h. After the reaction was completed as checked by TLC analysis, the solvent was removed by rotary evaporation. The resulting residue was diluted with $CHCl_3$. The mixture was filtered through a $MgSO_4$ pad. The solution obtained was sequentially washed with HCl (aq 10%) and brine. The organic layer was dried over $MgSO_4$ and concentrated under vacuum to give crude **33**, which was further purified by silica flash column chromatography (hexanes/CH_2Cl_2, 1:4) to yield compound **33** (233 mg, 0.243 mmol, 76%) as a yellow solid. Mp 185–186 °C; IR (KBr) 3032, 2943, 2891, 2864, 2210, 2148, 1731, 1631, 1597, 1567, 1489 cm^{-1}; ^{1}H NMR ($CDCl_3$, 500 MHz) δ 8.02 (dd, J=8.0, 1.0 Hz, 2H), 7.92 (br s, 2H), 7.75 (d, J=16.5 Hz, 2H), 7.70 (d, J=7.0 Hz, 2H), 7.56 (s, 4H), 7.54–7.51 (m, 4H), 7.44–7.42 (m, 4H), 7.24 (d, J=16.5 Hz, 2H), 4.00 (s, 6H), 1.21 (s, 42H); ^{13}C NMR ($CDCl_3$, 125 MHz) δ 166.8, 139.4, 137.1, 134.3, 133.4, 132.1, 132.0, 130.79, 130.68, 130.4, 128.4, 128.7, 127.4, 126.3, 123.74, 123.70, 122.8, 105.3, 98.3, 94.3, 90.1, 52.5, 19.0, 11.6; HRMS (CI) m/z calcd for $C_{64}H_{70}O_4Si_2$ 958.4813, found 959.5306 $[M+H]^+$.

7.19. Synthesis of OPE/OPV 34

To a solution of compound **33** (233 mg, 0.243 mmol) in THF (8 mL) was added TBAF (0.1 mL, 1 M in THF, 0.1 mmol). The mixture was stirred at rt for 5 min, then the solvent was removed by rotary evaporation. The residue was dissolved in $CHCl_3$ and sequentially washed with HCl (aq 10%) and brine. The organic layer dried over $MgSO_4$. Filtration to remove $MgSO_4$ followed by evaporation under vacuum afforded crude product **34**, which was purified with silica flash column chromatography (hexanes/CH_2Cl_2, 9:1) to yield compound **34** as a yellow solid (143 mg, 0.221 mmol, 91%). Mp >300 °C (dec); IR (KBr) 3290, 3029, 2953, 2920, 2850, 2212, 2099, 1724, 1667, 1646, 1598, 1565, 1489 cm^{-1}; ^{1}H NMR ($CDCl_3$, 500 MHz) δ 8.02 (d, J=8.5 Hz, 2H), 7.92 (d, J=1.5 Hz, 2H), 7.69 (d, J=8.5 Hz, 2H), 7.65 (d, J=16.0 Hz, 2H), 7.59 (s, 4H), 7.55–7.52 (m, 4H), 7.44–7.41 (m, 4H), 7.24 (d, J=17.0 Hz, 2H), 3.40 (s, 6H), 3.51 (s, 2H); ^{13}C NMR ($CDCl_3$, 125 MHz) δ 166.8, 139.7, 137.1, 134.4, 133.5, 132.0, 131.1, 130.8, 130.4, 128.4, 128.0, 127.5, 126.0, 124.2, 123.6, 121.3 (of the 16 aromatic and alkenyl carbons, one coincidental peak not observed), 94.0, 90.2, 84.0, 82.0, 52.5; HRMS (CI) m/z calcd for $C_{46}H_{30}O_4$ 646.2144 found 647.2826 $[M+H]^+$.

7.20. Synthesis of D-A substituted short H-mer 29 (*SH*-1,3-(COOMe)$_2$-2,4-(NMe$_2$)$_2$)

To an oven-dried round-bottom flask protected under a N_2 atmosphere were charged compound **34** (47 mg, 0.073 mmol), 4-iodo-*N*,*N*-dimethylaniline (36 mg, 0.15 mmol), $PdCl_2(PPh_3)_2$ (5.1 mg, 0.0072 mmol), CuI (2.8 mg, 0.015 mmol), piperidine (2.5 mL), and dry THF (2.5 mL). The solution was degassed by N_2 bubbling at rt for 5 min and then stirred at 30 °C under N_2 protection for 12 h. After the reaction was completed as checked by TLC analysis, the solvent was removed by rotary evaporation. The resulting residue was diluted with $CHCl_3$. The mixture was filtered through a $MgSO_4$ pad. The solution obtained was sequentially

washed with HCl (aq 10%) and brine. The organic layer was dried over $MgSO_4$ and concentrated under vacuum to give crude **29**, which was purified by silica flash column chromatography (CH_2Cl_2) to yield compound **29** (30 mg, 0.034 mmol, 47%) as a yellow solid. Mp 225–226 °C; IR (KBr) 2960, 2930, 2860, 2195, 1728, 1609, 1524, 1488, 1464 cm^{-1}; ^1H NMR ($CDCl_3$, 500 MHz) δ 8.01 (d, J=7.5 Hz, 2H), 7.91 (s, 2H), 7.76 (d, J=16.5 Hz, 2H), 7.69 (d, J=8.5 Hz, 2H), 7.61 (s, 4H), 7.54–7.47 (m, 8H), 7.43–7.39 (m, 4H), 7.28 (d, J=16.5 Hz, 2H), 6.70 (d, J=9.0 Hz, 4H), 4.00 (s, 6H), 3.00 (s, 12H); ^{13}C NMR ($CDCl_3$, 125 MHz) δ 166.9, 150.5, 138.5, 137.3, 134.3, 132.9, 132.4, 131.98, 131.95, 130.8, 130.48, 130.43, 128.2, 127.4, 126.6, 123.9, 123.6, 122.6, 112.1, 109.9 (of the 20 aromatic and alkenyl carbons, one coincidental peak not observed), 98.2, 94.6, 89.7, 86.3, 52.5, 40.4; HRMS (CI) m/z calcd for $C_{62}H_{48}N_2O_4$ 884.3614, found 885.3608 $[M+H]^+$.

7.21. Synthesis of long OPE/OPV H-mer 36 (*LH*)

Compound **16** (16 mg, 0.044 mmol), **35** (106 mg, 0.174 mmol), $PdCl_2(PPh_3)_2$ (6.11 mg, 0.00870 mmol), and CuI (3.31 mg, 0.0174 mmol) were added to Et_3N (8 mL). The solution was degassed by N_2 bubbling at rt for 5 min and then stirred for 4 h at rt, then heated to 50 °C under stirring and N_2 protection for 20 h. After the reaction was completed as checked by TLC analysis, the solvent was removed by rotary evaporation. The resulting residue was diluted with $CHCl_3$. The mixture was filtered through a $MgSO_4$ pad. The solution obtained was sequentially washed with HCl (aq 10%) and brine. The organic layer was dried over $MgSO_4$ and concentrated under vacuum to give crude **36**, which was further purified by silica flash column chromatography (hexanes/CH_2Cl_2, 7:3) to yield compound **36** (36 mg, 0.016 mmol, 36%) as a colorless oil. IR (KBr) 2956, 2925, 2854, 2153, 1698, 1683, 1650, 1635, 1558, 1539, 1504, 1470, 1415 cm^{-1}; ^1H NMR ($CDCl_3$, 500 MHz) δ 7.90 (s, 2H), 7.78 (d, J=16.0 Hz, 2H), 7.58 (s, 4H), 7.54 (d, J=8.5 Hz, 2H), 7.40 (d, J=8.5 Hz, 2H), 7.27 (d, J=16.0 Hz, 2H), 7.01 (s, 2H), 7.00 (s, 4H), 6.99 (s, 2H), 4.06–3.99 (m, 16H), 1.90–1.18 (m, 128H), 0.92–0.83 (m, 24H), 0.30 (s, 18H), 0.29 (s, 18H); ^{13}C NMR ($CDCl_3$, 125 MHz) δ 154.4, 153.81, 153.8, 139.0, 137.3, 132.8, 130.7, 130.3, 128.1, 127.5, 126.5, 123.7, 122.5, 117.7, 117.6, 117.11, 117.06, 114.4, 114.2, 101.3, 100.6, 100.5, 94.9, 93.5, 93.1, 87.9, 70.0, 69.9, 69.8, 32.1, 29.9, 29.83, 29.77, 29.7, 29.64, 29.29.62, 29.6, 29.4, 26.3, 26.1, 22.9, 14.3, 0.19; HRMS (MALDI-TOF) m/z calcd for $C_{154}H_{226}O_8Si_4$ 2315.6388, found 2315.7135 $[M]^+$.

7.22. Synthesis of 4-((2,5-bis(decyloxy)-4-((trimethylsilyl) ethynyl)phenyl)ethynyl)benzonitrile (40)

Compound **39** (100 mg, 0.787 mmol), **35** (484 mg, 0.787 mmol), $PdCl_2(PPh_3)_2$ (27 mg, 0.039 mmol), and CuI (15 mg, 0.079 mmol) were added to Et_3N (20 mL). The solution was bubbled by N_2 at rt for 5 min and then stirred at rt for 4 h under N_2 protection. After the reaction was completed as checked by TLC analysis, the solvent was removed by rotary evaporation. The resulting residue was diluted with $CHCl_3$. The mixture was filtered through a $MgSO_4$ pad. The solution obtained was sequentially washed with HCl (aq 10%) and brine. The organic layer was dried over $MgSO_4$ and concentrated under vacuum to give crude **40**, which was further purified by silica flash column chromatography (hexanes/CH_2Cl_2, 4:1) to yield compound **40** (482 mg, 0.787 mmol, 100%) as a colorless oil. IR (KBr) 2925, 2854, 2228, 2212, 2153, 1604, 1508, 1493, 1468, 1412, 1384 cm^{-1}; ^1H NMR ($CDCl_3$, 500 MHz) δ 7.63 (d, J=8.0 Hz, 2H), 7.59 (d, J=8.0 Hz, 2H), 6.96 (s, 2H), 4.01–3.97 (m, 4H), 1.84–1.80 (m, 4H), 1.55–1.49 (m, 4H), 1.37–1.28 (m, 24H), 0.90–0.87 (m, 6H); ^{13}C NMR ($CDCl_3$, 125 MHz) δ 154.3, 154.0, 132.2, 132.1, 128.6, 118.7, 117.3, 117.1, 115.1, 113.1, 111.6, 101.1, 101.0, 93.2, 90.7, 69.8, 69.7, 32.1, 29.9, 29.8, 29.6, 29.58, 29.54, 29.5, 26.2, 22.9, 14.3, 0.14; HRMS (CI) m/z calcd for $C_{40}H_{57}NO_2Si$ 611.4159, found 612.4176 $[M+H]^+$.

7.23. Synthesis of 4-((2,5-bis(decyloxy)-4-ethynylphenyl) ethynyl)benzonitrile (41)

To a solution of compound **40** (428 mg, 0.699 mmol) in MeOH/THF (10 mL, 1:1) was added K_2CO_3 (100 mg, 0.724 mmol). The mixture was stirred at rt for 30 min, then the reaction solvent was removed by rotary evaporation. The residue was diluted with EtOAc and sequentially washed with HCl (aq 10%) and brine. The organic layer was dried over $MgSO_4$ and concentrated under vacuum to afford crude **41**, which was further purified by silica flash column chromatography (hexanes/CH_2Cl_2, 4:1) to yield compound **41** (333 mg, 0.617 mmol, 88%) as a colorless oil. IR (KBr) 3290, 3256, 2925, 2852, 2226, 2155, 2102, 1639, 1605, 1508, 1494, 1466, 1409, 1387 cm^{-1}; ^1H NMR ($CDCl_3$, 500 MHz) δ 7.64 (d, J=8.5 Hz, 2H), 7.60 (d, J=8.5 Hz, 2H), 7.00 (s, 1H), 6.99 (s, 1H), 4.03–3.99 (m, 4H), 3.37 (s, 1H), 1.86–1.80 (m, 4H), 1.55–1.46 (m, 4H), 1.38–1.26 (m, 24H), 0.90–0.87 (m, 6H); ^{13}C NMR ($CDCl_3$, 125 MHz) δ 154.3, 153.9, 132.21, 132.17, 128.5, 118.7, 117.8, 117.1, 113.9, 113.5, 111.7, 93.2, 90.5, 83.0, 80.0, 69.9, 69.7, 32.10, 32.09, 29.9, 29.8, 29.6, 29.53, 29.46, 29.3, 26.2, 26.1, 22.9, 14.3; HRMS (CI) m/z calcd for $C_{37}H_{49}NO_2$ 539.3763, found 540.3759 $[M+H]^+$.

7.24. Synthesis of ((2,5-bis(decyloxy)-4-((4-methoxyphenyl) ethynyl)phenyl)ethynyl)trimethylsilane (45)

Compound **44** (108 mg, 0.818 mmol), **35** (500 mg, 0.818 mmol), $PdCl_2(PPh_3)_2$ (14 mg, 0.020 mmol), and CuI (7.8 mg, 0.041 mmol) were added to Et_3N (15 mL). The solution was bubbled with N_2 at rt for 5 min and then stirred under N_2 protection overnight. After the reaction was completed as checked by TLC analysis, the solvent was removed by rotary evaporation. The resulting residue was diluted with $CHCl_3$. The mixture was filtered through a $MgSO_4$ pad. The solution obtained was sequentially washed with HCl (aq 10%) and brine. The organic layer was dried over $MgSO_4$ and concentrated under vacuum to give crude **45**, which was further purified by silica flash column chromatography (hexanes/CH_2Cl_2, 17:1) to yield compound **45** (463 mg, 0.750 mmol, 92%) as a colorless oil. IR (KBr) 2955, 2923, 2854, 2209, 2153, 1607, 1570, 1514, 1497, 1468, 1442, 1410, 1388 cm^{-1}; ^1H NMR ($CDCl_3$, 500 MHz) δ 7.46 (d, J=9.5 Hz, 2H), 6.94 (s, 1H), 6.93 (s, 1H), 6.86 (d, J=9.5 Hz, 2H), 3.40–3.96 (m, 4H), 3.82 (s, 3H), 1.83–1.78 (m, 4H), 1.53–1.50 (m, 4H), 1.36–1.25 (m, 24H), 0.90–0.86 (m, 6H), 0.26 (s, 9H); ^{13}C NMR ($CDCl_3$, 125 MHz) δ 159.8, 154.4, 153.5, 133.2, 117.5, 116.9, 115.8, 115.0, 114.3, 114.1, 113.5, 101.5, 99.9, 95.2, 84.8, 69.8, 69.6, 55.3, 34.8, 32.1, 29.85, 29.80, 29.77, 29.63, 29.56, 29.53, 26.3, 26.2, 22.9, 14.3, 0.16; HRMS (CI) m/z calcd for $C_{40}H_{60}O_3Si$ 616.4321, found 617.4386 $[M+H]^+$.

7.25. Synthesis of 1,4-bis(decyloxy)-2-ethynyl-5-((4-methoxyphenyl)ethynyl)benzene (46)

To a solution of compound **45** (463 mg, 0.750 mmol) in MeOH/$CHCl_3$ (16 mL, 1:1) was added K_2CO_3 (200 mg, 1.44 mmol). The mixture was stirred at rt for 2 h, then the reaction solvent was removed by rotary evaporation. The residue was diluted with CH_2Cl_2 and sequentially washed with HCl (aq 10%) and brine. The organic layer was dried over $MgSO_4$ and concentrated under vacuum to afford crude **46**, which was further purified by silica flash column chromatography (hexanes/CH_2Cl_2, 17:1) to yield compound **46** (392 mg, 0.72 mmol, 96%) as a white solid. Mp 40–41 °C; IR (KBr) 3293, 2959, 2920, 2851, 2215, 2152, 1610, 1569, 1516, 1499, 1471, 1410, 1392 cm^{-1}; ^1H NMR ($CDCl_3$, 500 MHz) δ 7.42 (d, J=11.0 Hz, 2H), 6.98 (s, 1H), 6.97 (s, 1H), 6.88 (d, J=11.0 Hz, 2H), 4.01–3.97 (m, 4H), 3.82 (s, 3H), 3.33 (s, 1H), 1.85–1.79 (m, 4H),

1.54–1.45 (m, 4H), 1.36–1.26 (m, 24H), 0.90–0.87 (m, 6H); ^{13}C NMR ($CDCl_3$, 125 MHz) δ 160.1, 154.6, 153.7, 133.5, 118.3, 117.2, 116.0, 115.6, 114.4, 112.6, 95.5, 84.9, 82.5, 80.5, 70.10, 70.05, 55.7, 32.35, 32.34, 30.1, 30.02, 30.0, 29.9, 29.8, 29.6, 26.5, 26.4, 23.1, 14.5; HRMS (CI) *m*/*z* calcd for $C_{37}H_{52}O_3$ 544.3916, found 545.4039 $[M+H]^+$.

7.26. Synthesis of A-substituted long OPE/OPV H-mer 47 (*LH*-(CN)$_4$)

Compound **41** (112 mg, 0.207 mmol), **14** (19 mg, 0.033 mmol), Pd(PPh_3)$_4$ (24 mg, 0.021 mmol), and CuI (7.8 mg, 0.041 mmol) were added to Et_3N (6 mL). The solution was bubbled with N_2 at rt for 5 min and then heated to 50 °C under stirring and N_2 protection for 17 h. After the reaction was completed as checked by TLC analysis, the solvent was removed by rotary evaporation. The resulting residue was diluted with $CHCl_3$. The mixture was filtered through a $MgSO_4$ pad. The solution obtained was sequentially washed with HCl (aq 10%) and brine. The organic layer was dried over $MgSO_4$ and concentrated under vacuum to give crude **47**, which was further purified by silica flash column chromatography (hexanes/CH_2Cl_2, 1:1) to yield compound **47** (47 mg, 0.019 mmol, 59%) as a yellow solid. Mp 134–135 °C; IR (KBr) 2924, 2853, 2226, 2207, 1693, 1663, 1552, 1533, 1514, 1467, 1417, 1385 cm^{-1}; ^{1}H NMR ($CDCl_3$, 500 MHz) δ 7.92 (s, 2H), 7.81 (d, *J*=15.5 Hz, 2H), 7.67–7.59 (m, 20H), 7.57 (d, *J*=8.5 Hz, 2H), 7.42 (dd, *J*=8.5, 1.5 Hz, 2H), 7.29 (d, *J*=15.5 Hz, 2H), 7.07 (s, 4H), 7.06 (s, 2H), 7.05 (s, 2H), 4.09–4.03 (m, 16H), 1.93–1.82 (m, 12H), 1.77–1.72 (m, 4H), 1.62–1.49 (m, 12H), 1.45–1.18 (m, 100H), 0.90–0.83 (m, 24H); ^{13}C NMR ($CDCl_3$, 125 MHz) δ 154.20, 154.17, 153.9, 153.8, 139.0, 137.3, 132.8, 132.3, 132.20. 132.18, 132.1, 130.7, 130.4, 128.61, 128.56, 128.0, 127.5, 126.6, 123.8, 122.5, 118.73, 118.69, 117.3, 117.2, 117.0, 116.9, 115.3, 115.0, 113.31, 113.28, 111.7, 111.6, 95.3, 94.0, 93.5, 93.4, 93.1, 90.8, 90.7, 87.9, 70.1, 69.9, 69.8, 32.1, 29.9, 29.8, 29.64, 29.61, 29.5, 29.4, 26.3, 26.1, 22.9, 14.3; HRMS (MALDI-TOF) *m*/*z* calcd for $C_{170}H_{206}N_4O_8$ 2431.5836, found 2432.7026 $[M+H]^+$.

7.27. Synthesis of D-substituted long OPE/OPV H-mer 48 (*LH*-(OMe)$_4$)

Compound **46** (113 mg, 0.207 mmol), **14** (19 mg, 0.32 mmol), Pd(PPh_3)$_4$ (25 mg, 0.022 mmol), and CuI (12 mg, 0.063 mmol) were added to Et_3N (8 mL). The solution was degassed by N_2 bubbling at rt for 5 min and then heated to 60 °C under stirring and N_2 protection for 18 h. After the reaction was completed as checked by TLC analysis, the solvent was removed by rotary evaporation. The resulting residue was diluted with $CHCl_3$. The mixture was filtered through a $MgSO_4$ pad. The solution obtained was sequentially washed with HCl (aq 10%) and brine. The organic layer was dried over $MgSO_4$ and concentrated under vacuum to give crude **48**, which was further purified by silica flash column chromatography (hexanes/CH_2Cl_2, 1:1) to yield compound **48** (45 mg, 0.018 mmol, 57%) as a yellow solid. Mp 98–99 °C; IR (KBr) 2953, 2923, 2853, 2204, 1608, 1515, 1498, 1466, 1417, 1383 cm^{-1}; ^{1}H NMR (CDCl3, 500 MHz) δ 7.91 (s, 2H), 7.81 (d, *J*=17.0 Hz, 2H), 7.60 (s, 4H), 7.55 (d, *J*=8.0 Hz, 2H), 7.50 (d, *J*=8.5 Hz, 4H), 7.48 (d, *J*=8.5 Hz, 4H), 7.40 (d, *J*=8.5 Hz, 2H), 7.28 (d, *J*=17.0 Hz, 2H), 7.06 (s, 2H), 7.05 (s, 4H), 7.03 (s, 2H), 6.89 (d, *J*=8.5 Hz, 4H), 6.86 (d, *J*=8.5 Hz, 4H), 4.08–4.02 (m, 16H), 3.84 (s, 1H), 3.82 (s, 1H), 1.91–1.82 (m, 12H), 1.77–1.71 (m, 4H), 1.61–1.51 (m, 12H), 1.43–1.17 (m, 100H), 0.90–0.82 (m, 24H); ^{13}C NMR ($CDCl_3$, 125 MHz) δ 159.91, 159.87, 154.02, 153.97, 153.7, 138.9, 137.3, 133.3, 132.7, 130.7, 130.2, 128.0, 127.5, 126.6, 123.8, 122.5, 117.24, 117.20, 117.1, 115.8, 115.2, 115.0, 114.20, 114.18, 113.7, 113.5, 95.5, 95.4, 94.7, 93.3, 88.0, 84.92, 84.89, 70.04, 69.95, 69.92, 69.9, 55.5, 55.47, 32.1, 29.9, 29.8, 29.7, 29.68, 29.65, 29.63, 29.58, 29.4, 22.9, 14.3; HRMS (MALDI-TOF) *m*/*z* calcd for $C_{170}H_{218}O_{12}$ 2451.6448, found 2453.0938 $[M+H]^+$.

7.28. Synthesis of A-substituted long OPE/OPV H-mer 50 (*LH*-(CHO)$_4$)

Compound **49** (125 mg, 0.230 mmol), **14** (25 mg, 0.036 mmol), Pd(PPh_3)$_4$ (15 mg, 0.013 mmol), and CuI (8.0 mg, 0.042 mmol) were added to Et_3N (8 mL). The solution was bubbled with N_2 at rt for 5 min and then stirred at rt under N_2 protection for 1 h. Afterward, the reaction was heated to 60 °C and stirred for 18 h under N_2 protection. After the reaction was completed as checked by TLC analysis, the solvent was removed by rotary evaporation. The resulting residue was diluted with $CHCl_3$. The mixture was filtered through a $MgSO_4$ pad. The solution obtained was sequentially washed with HCl (aq 10%) and brine. The organic layer was dried over $MgSO_4$ and concentrated under vacuum to give crude **50**, which was further purified by silica flash column chromatography (hexanes/EtOAc, 7:3) to yield compound **50** (60 mg, 0.025 mmol, 68%) as a yellow solid. Mp 103–104 °C; IR (KBr) 2924, 2853, 2727, 2207, 1703, 1600, 1560, 1513, 1496, 1467, 1417, 1386 cm^{-1}; ^{1}H NMR ($CDCl_3$, 500 MHz) δ 10.03 (s, 2H), 10.00 (s, 2H), 7.91 (s, 2H), 7.88 (d, *J*=8.5 Hz, 4H), 7.83 (d, *J*=8.5 Hz, 4H), 7.81 (d, *J*=17.5 Hz, 2H), 7.68 (d, *J*=9.0 Hz, 4H), 7.65 (d, *J*=8.5 Hz, 4H), 7.60 (s, 4H). 7.56 (d, *J*=8.5 Hz, 2H), 7.41 (d, *J*=8.0 Hz, 2H), 7.28 (d, *J*=18 Hz, 2H), 7.03 (s, 2H), 7.06 (s, 4H), 7.05 (s, 2H), 4.09–4.03 (m, 16H, OCH2), 1.92–1.17 (m, 128H), 0.88–0.79 (m, 24H); ^{13}C NMR ($CDCl_3$, 125 MHz) δ 191.53, 191.47, 154.19, 154.16, 153.93, 153.86, 139.0, 137.3, 135.61, 135.57, 132.8, 132.23, 132.20, 130.7, 130.3, 130.0, 129.9, 129.8, 129.7, 128.0, 127.5, 126.6, 123.8, 122.5, 117.4, 117.2, 117.1, 117.0, 115.1, 114.8, 113.7, 113.6, 95.3, 94.4, 94.3, 93.9, 93.1, 90.41, 90.39, 87.9, 70.1, 69.9, 69.8, 32.1, 29.9, 29.8, 29.78, 29.7, 29.6, 29.4, 26.35, 26.31, 26.1, 22.9, 14.3; HRMS (MALDI-TOF) *m*/*z* calcd for $C_{170}H_{210}O_{12}$ 2443.5822, found 2444.7471 $[M+H]^+$.

7.29. Synthesis of OPE 51

Compound **12** (32 mg, 0.10 mmol), **41** (55.6 mg, 0.103 mmol), $PdCl_2(PPh_3)_2$ (3.6 mg, 0.0051 mmol), and CuI (1.96 mg, 0.0103 mmol) were added to Et_3N (6 mL). The solution was bubbled with N_2 at rt for 5 min and then stirred at rt under N_2 protection for 3 h. After the reaction was completed as checked by TLC analysis, the solvent was removed by rotary evaporation. The resulting residue was diluted with $CHCl_3$. The mixture was filtered through a $MgSO_4$ pad. The solution obtained was sequentially washed with HCl (aq 10%) and brine. The organic layer was dried over $MgSO_4$ and concentrated under vacuum to give crude **51**, which was further purified by silica flash column chromatography (hexanes/CH_2Cl_2, 7:3) to yield compound **51** (60 mg, 0.083 mmol, 81%) as a white solid. Mp 82–83 °C; IR (KBr) 2918, 2851, 2207, 1690, 1631, 1603, 1583, 1552, 1533, 1513, 1497, 1469, 1420 cm^{-1}; ^{1}H NMR ($CDCl_3$, 500 MHz) δ 10.66 (s, 1H), 8.07 (d, *J*=1.5 Hz, 1H), 7.69 (dd, *J*=8.0, 1.5 Hz, 1H), 7.64 (d, *J*=8.5 Hz, 2H), 7.60 (d, *J*=8.5 Hz, 2H), 7.49 (d, *J*=8.0 Hz, 1H), 7.02 (s, 1H), 7.01 (s, 1H), 4.05–4.01 (m, 4H), 1.89–1.83 (m, 4H), 1.60–1.46 (m, 4H), 1.30–1.26 (m, 24H), 0.89–0.86 (m, 6H); ^{13}C NMR ($CDCl_3$, 125 MHz) δ 190.9, 154.3, 154.0, 137.2, 136.8, 134.3, 132.24, 132.20, 130.3, 128.5, 125.9, 123.4, 118.7, 116.7, 116.4, 114.1, 113.5, 111.8, 94.3, 93.8, 90.5, 90.2, 69.8, 69.6, 32.1, 29.9, 29.82, 29.76, 29.6, 29.5, 29.4, 26.3, 22.9,14.3; HRMS (CI) *m*/*z* calcd for $C_{44}H_{52}BrNO_3$ 721.3131, found 722.3139 $[M+H]^+$.

7.30. Synthesis of OPE 52

Compound **51** (61 mg, 0.084 mmol), **46**(142 mg, 0.261 mmol), Pd(PPh_3)$_4$ (15 mg, 0.13 mmol), and CuI (5.0 mg, 0.026 mmol) were added to Et_3N (10 mL). The solution was bubbled with N_2 at rt for 5 min, stirred at rt for 3 h, and then heated to 60 °C under stirring and N_2 protection for 4 h. After the reaction was completed as checked by TLC analysis, the solvent was removed by rotary

evaporation. The resulting residue was diluted with $CHCl_3$. The mixture was filtered through a $MgSO_4$ pad. The solution obtained was sequentially washed with HCl (aq 10%) and brine. The organic layer was dried over $MgSO_4$ and concentrated under vacuum to give crude **52**, which was further purified by silica flash column chromatography (hexanes/CH_2Cl_2, 3:2) to yield compound **52** (80 mg, 0.067 mmol, 80%) as a yellow solid. Mp 128–129 °C; IR (KBr) 2922, 2851, 2224, 2208, 1696, 1649, 1604, 1557, 1515, 1486, 1467, 1417, 1387 cm^{-1}; ^1H NMR ($CDCl_3$, 500 MHz) δ 10.73 (s, 1H), 8.11 (d, J=2.0 Hz, 1H), 7.70 (dd, J=8.5, 2.0 Hz, 1H), 7.66 (d, J=8.5 Hz, 2H), 7.62 (d, J=8.5 Hz, 2H), 7.61 (d, J=8.5 Hz, 1H), 7.49 (d, J=8.5 Hz, 2H), 7.05 (s, 1H), 7.03 (s, 1H), 7.022 (s, 1H), 7.016 (s, 1H), 6.70 (d, J=8.5 Hz, 2H), 4.07–4.04 (m, 4H), 4.07–4.04 (m, 8H), 3.85 (s, 3H), 1.91–1.84 (m, 8H), 1.56–1.48 (m, 8H), 1.40–1.27 (m, 48H), 0.91–0.86 (m, 12H); ^{13}C NMR ($CDCl_3$, 125 MHz) δ 191.5, 159.9, 154.3, 154.1, 154.0, 153.6, 136.2, 136.1, 133.3, 133.0, 132.22, 132.19, 130.3, 128.5, 126.2, 124.5, 118.7, 117.2, 116.9, 116.7, 116.4, 115.7, 115.5, 114.2, 114.0, 113.8, 112.9, 111.7, 95.6, 94.8, 93.7, 93.4, 91.2, 90.7, 89.7, 84.8, 69.9, 69.8, 69.6, 55.5, 32.1, 29.9, 29.83, 29.78, 29.7, 29.6, 29.56, 29.53, 29.5, 26.3, 22.9, 14.3; HRMS (MALDI-TOF) m/z calcd for $C_{81}H_{103}NO_6$ 1185.7785, found 1186.0105 $[M+H]^+$.

7.31. Synthesis of OPE 53

Compound **12** (32.0 mg, 0.103 mmol), **46** (55.6 mg, 0.103 mmol), $PdCl_2(PPh_3)_2$ (3.6 mg, 0.0051 mmol), and CuI (1.96 mg, 0.0103 mmol) were added to Et_3N (8 mL). The solution was bubbled with N_2 at rt for 5 min and then stirred at rt under N_2 protection for 8 h. After the reaction was completed as checked by TLC analysis, the solvent was removed by rotary evaporation. The resulting residue was diluted with $CHCl_3$. The mixture was filtered through a $MgSO_4$ pad. The solution obtained was sequentially washed with HCl (aq 10%) and brine. The organic layer was dried over $MgSO_4$ and concentrated under vacuum to give crude **53**, which was further purified by silica flash column chromatography (hexanes/CH_2Cl_2, 7:3) to yield compound **53** (21 mg, 0.029 mmol, 28%) as a white solid. Mp 75–76 °C; IR (KBr) 2920, 2872, 2852, 2203, 1692, 1600, 1581, 1568, 1514, 1499, 1466, 1418 cm^{-1}; ^1H NMR ($CDCl_3$, 500 MHz) δ 10.68 (s, 1H), 8.08 (d, J=1.5 Hz, 1H), 7.70 (dd, J=8.5, 1.5 Hz, 1H), 7.50 (d, J=8.5 Hz, 2H), 7.49 (d, J=8.5 Hz, 2H), 7.02 (s, 1H), 7.01 (s, 1H), 6.90 (d, J=8.5 Hz, 1H), 4.06–4.02 (m, 4H), 3.85 (s, 3H), 1.90–1.84 (m, 4H), 1.59–1.47 (m, 4H), 1.42–1.27 (m, 24H), 0.90–0.87 (m, 6H); ^{13}C NMR ($CDCl_3$, 125 MHz) δ 191.3, 160.2, 154.7, 153.8, 137.4, 137.0, 134.5, 133.5, 130.5, 126.4, 123.3, 117.1, 116.5, 116.3, 115.8, 114.4, 112.1, 96.2, 95.0, 89.7, 85.0, 70.2, 69.7, 55.7, 32.3, 30.1, 30.05, 30.01, 30.0, 29.9, 29.8, 29.76, 29.70, 26.5, 23.1, 14.5; HRMS (CI) m/z calcd for $C_{44}H_{55}BrO_4$ 726.3284, found 727.3430 $[M+H]^+$.

7.32. Synthesis of OPE 54

Compound **53** (21 mg, 0.029 mmol), **41** (31.2 mg, 0.0578 mmol), $PdCl_2(PPh_3)_2$ (2.0 mg, 0.0029 mmol), and CuI (1.1 mg, 0.0058 mmol) were added to Et_3N (6 mL). The solution was bubbled with N_2 at rt for 5 min and then stirred for 3 h at rt and then heated to 60 °C under stirring and N_2 protection for 5 h. After the reaction was completed as checked by TLC analysis, the solvent was removed by rotary evaporation. The resulting residue was diluted with chloroform. The mixture was filtered through a $MgSO_4$ pad. The solution obtained was sequentially washed with HCl (aq 10%) and brine. The organic layer was dried over MgSO4 and concentrated under vacuum to give crude **54**, which was further purified by silica flash column chromatography (hexanes/CH_2Cl_2, 13:7) to yield compound **54** (24 mg, 0.020 mmol, 71%) as a yellow solid. Mp 98–99 °C; IR (KBr) 2954, 2924, 2852, 2204, 1694, 1632, 1553, 1535, 1516, 1484, 1468, 1453, 1416 cm^{-1}; ^1H NMR ($CDCl_3$, 500 MHz) δ 10.73 (s, 1H), 8.09 (d, J=1.0 Hz, 1H), 7.68 (dd, J=8.0, 1.0 Hz, 1H), 7.64 (d, J=8.0 Hz, 2H), 7.60 (d, J=8.0 Hz, 2H), 7.60 (d, J=8.0 Hz, 1H), 7.48 (d, J=8.5 Hz, 2H), 7.02 (s, 1H), 7.01 (br, 3H), 6.89 (d, J=8.5 Hz, 2H), 4.05–4.03 (m, 4H), 3.83 (s, 3H), 1.90–1.82 (m, 8H), 1.58–1.47 (m, 8H), 1.39–1.25 (m, 48H), 0.89–0.85 (m, 12H); ^{13}C NMR ($CDCl_3$, 125 MHz) δ 191.7, 160.0, 154.5, 154.1, 153.9, 153.6, 136.2, 136.0, 133.3, 133.0, 132.3, 132.2, 130.4, 128.6, 126.8, 123.9, 118.8, 117.1, 117.06, 117.0, 116.3, 116.0, 115.7, 114.6, 114.2, 113.5, 112.1, 111.7, 96.0, 95.4, 94.2, 93.5, 90.7, 90.4, 89.0, 84.8, 70.00, 69.95, 69.8, 69.6, 55.5, 32.1, 29.9, 29.8, 29.79, 29.7, 29.6, 29.5, 26.3, 22.9, 14.3; HRMS (MALDI-TOF) m/z calcd for $C_{81}H_{103}NO_6$ 1185.7785, found 1186.0105 $[M+H]^+$.

7.33. Synthesis of D-A substituted long OPE/OPV H-mer 55 (*LH*-1,3-$(CN)_2$-2,4-$(OMe)_2$)

To an oven-dried round-bottom flask protected under N_2 atmosphere were added compound **13** (12.8 mg, 0.337 mmol), NaH (2.02 mg, 0.0843 mmol), and dry THF (8 mL). Upon gentle heating at 50 °C, the solution gradually turned into a pink color. Aldehyde **52** (80 mg, 0.067 mmol) dissolved in THF (5 mL) was added in small portions over a period of 1 h through a syringe. The reaction was kept under stirring and heating for another 2 h before workup. The small excess NaH was carefully quenched with H_2O and the mixture was extracted with $CHCl_3$ three times. The organic layer was washed with brine, dried over $MgSO_4$, and concentrated to form a yellow solid. The yellow solid was purified by silica flash column chromatography (hexanes/CH_2Cl_2, 1:1) to give compound **55** (35 mg, 0.014 mmol, 21%) as a yellow solid. Mp 126–127 °C; IR (KBr) 2923, 2853, 2227, 2206, 1634, 1605, 1557, 1514, 1496, 1468, 1417, 1393 cm^{-1}; ^1H NMR ($CDCl_3$, 500 MHz) δ 7.91 (s, 2H), 7.80 (d, J=16.5 Hz, 2H), 7.62 (d, J=8.0 Hz, 4H), 7.60 (s, 4H), 7.58 (d, J=8.0 Hz, 4H), 7.55 (d, J=7.0 Hz, 2H), 7.50 (d, J=8.5 Hz, 4H), 7.43 (d, J=7.0 Hz, 2H), 7.28 (d, J=16.5 Hz, 2H), 7.06 (s, 2H), 7.05 (s, 2H), 7.041 (s, 2H), 7.036 (s, 2H), 6.90 (d, J=8.5 Hz, 4H), 4.08–4.02 (m, 16H), 3.85 (s, 6H), 1.90–1.82 (m, 12H), 1.77–1.71 (m, 4H), 1.61–1.49 (m, 12H), 1.42–1.17 (m, 100H), 0.90–0.82 (m, 24H); ^{13}C NMR ($CDCl_3$, 125 MHz) δ 159.9, 154.2, 154.0, 153.8, 153.7, 139.0, 137.3, 133.3, 132.8, 132.22, 132.16, 130.8, 130.3, 128.6, 128.0, 127.5, 126.6, 124.1, 122.2, 118.7, 117.4, 117.3, 117.1, 116.9, 115.8, 115.4, 115.1, 114.2, 113.4, 113.2, 111.6, 95.5, 94.6, 94.1, 93.5, 92.9, 90.8, 88.3, 84.8, 70.2, 70.0, 69.9, 69.8, 55.5, 32.1, 29.9, 29.8, 29.69, 29.66, 29.64, 29.58, 29.4, 26.3, 26.1, 22.9, 14.3; HRMS (MALDI-TOF) m/z calcd for $C_{170}H_{212}N_2O_{10}$ 2441.6142, found 2442.9568 $[M+H]^+$.

7.34. Synthesis of D-A substituted long OPE/OPV H-mer 56 (*LH*-2,4-$(CN)_2$-1,3-$(OMe)_2$)

To an oven-dried round-bottom flask protected under a N_2 atmosphere were added compound **13** (2.88 mg, 0.00761 mmol), NaH (0.36 mg, 0.0152 mmol), and dry THF (6 mL). Upon gentle heating at 50 °C, the solution gradually turned into a pink color. Aldehyde **54** (18 mg, 0.015 mmol) dissolved in THF (5 mL) was added in small portions over a period of 1 h through a syringe. The reaction was kept under stirring and heating for another 4 h before workup. The small excess NaH was carefully quenched with H_2O and the mixture was extracted three times with $CHCl_3$. The organic layer was washed with brine, dried over $MgSO_4$, and concentrated to form a yellow solid. The yellow solid was purified by silica flash column chromatography (hexanes/CH_2Cl_2, 1:1) to give compound **56** (11 mg, 0.0045 mmol, 59%) as a yellow solid. Mp 121–122 °C; IR (KBr) 2924, 2854, 2226, 2202, 1649, 1635, 1558, 1540, 1514, 1469, 1418, 1385 cm^{-1}; ^1H NMR ($CDCl_3$, 500 MHz) δ 7.91 (s, 2H), 7.80 (d, J=15.5 Hz, 2H), 7.66 (d, J=8.5 Hz, 4H), 7.62 (d, J=8.5 Hz, 4H), 7.60 (s, 4H), 7.55 (d, J=8.0 Hz, 2H), 7.48 (d, J=8.5 Hz, 4H), 7.41 (d, J=8.0 Hz, 2H), 7.28 (d, J=15.5 Hz, 2H), 7.07 (s, 2H), 7.06 (s, 2H), 7.04 (s, 4H), 6.87 (d, J=8.5 Hz, 4H), 4.09–4.02 (m, 16H), 3.83 (s, 6H), 1.91–1.83 (m, 12H), 1.76–1.71 (m, 4H), 1.61–1.51 (m, 12H), 1.44–1.17 (m, 100H), 0.90–0.82 (m, 24H); ^{13}C NMR ($CDCl_3$, 125 MHz) δ 159.9,

154.2, 154.0, 153.8, 153.7, 139.0, 137.3, 133.3, 132.8, 132.3, 132.2, 130.7, 130.3, 128.7, 128.1, 127.5, 126.6, 123.5, 122.8, 118.8, 117.22, 117.19, 117.0, 115.8, 115.24, 115.17, 114.2, 113.6, 113.2, 111.6, 95.55, 95.47, 93.5, 93.4, 93.2, 90.8, 87.7, 84.9, 70.0, 69.96, 69.8, 55.5, 32.1, 29.9, 29.83, 29.79, 29.71, 29.66, 29.63, 29.58, 29.4, 26.3, 26.2, 22.9, 14.3; HRMS (MALDI-TOF) *m/z* calcd for $C_{170}H_{212}N_2O_{10}$ 2441.6142, found 2442.6895 $[M+H]^+$.

7.35. Synthesis of Z-shaped OPE/OPV 57

Compound **14** (35.5 mg, 0.0652 mmol), **46** (22.5 mg, 0.0326 mmol), $PdCl_2(PPh_3)_2$ (2.3 mg, 0.0033 mmol), and CuI (1.2 mg, 0.0065 mmol) were added to Et_3N (8 mL). The solution was bubbled with N_2 at rt for 5 min and then was stirred at rt under N_2 protection for 7 h. After the reaction was completed as checked by TLC analysis, the solvent was removed by rotary evaporation. The resulting residue was diluted with $CHCl_3$. The mixture was filtered through a $MgSO_4$ pad. The solution obtained was sequentially washed with HCl (aq 10%) and brine. The organic layer was dried over $MgSO_4$ and concentrated under vacuum to give crude **57**, which was further purified by silica flash column chromatography (hexanes/CH_2Cl_2, 7:3) to yield compound **57** (24 mg, 0.016 mmol, 48%) as a yellow solid. Mp 138–139 °C; IR (KBr) 2959, 2924, 2853, 2206, 1636, 1620, 1576, 1559, 1540, 1514, 1459, 1417, 1384 cm^{-1}; ^1H NMR ($CDCl_3$, 500 MHz) δ 7.86 (d, J=2.0 Hz, 2H), 7.74 (d, J=16 Hz, 2H), 7.58 (s, 4H), 7.48 (d, J=8.5 Hz, 4H), 7.42 (d, J=8.5 Hz, 2H), 7.36 (dd, J=16.0, 2 Hz, 2H), 7.21 (d, J=16.0 Hz, 2H), 7.05 (s, 2H), 7.02 (s, 2H), 6.87 (d, J=8.5 Hz, 4H), 4.02 (t, J=6.5 Hz, 8H), 3.83 (s, 6H), 1.87–1.81 (m, 4H), 1.74–1.69 (m, 4H), 1.56–1.50 (m, 4H), 1.38–1.16 (m, 52H), 0.87 (t, J=6.0 Hz, 6H), 0.85 (t, J=6.0 Hz, 6H); ^{13}C NMR ($CDCl_3$, 125 MHz) δ 160.1, 154.2, 153.9, 140.9, 137.4, 134.2, 133.5, 131.3, 130.6, 128.1, 127.8, 126.3, 123.1, 121.9, 117.37, 117.35, 116.0, 115.5, 114.4, 113.7, 95.7, 92.9, 92.7, 85.1, 70.23, 70.18, 55.7, 32.33, 32.31, 30.1, 30.05, 30.03, 30.0, 29.91, 29.85, 29.8, 29.6, 26.6, 26.4, 23.1, 14.5; MALDI-TOF MS (+eV) *m/z* calcd for $C_{96}H_{116}Br_2O_6$ 1522.7152, found 1523.7930 $[M+H]^+$.

7.36. Synthesis of D-A substituted long OPE/OPV H-mer 58 (*LH*-1,3-(OMe)$_2$-2,4-(CHO)$_2$)

Compound **57** (24 mg, 0.016 mmol), **49** (34 mg, 0.063 mmol), $PdCl_2(PPh_3)_2$ (1.1 mg, 0.0016 mmol), and CuI (0.59 mg, 0.0031 mmol) were added to Et_3N (6 mL). The solution was bubbled with N_2 at rt for 5 min and then stirred at 65 °C under N_2 protection for 12 h. After the reaction was completed as checked by TLC analysis, the solvent was removed by rotary evaporation. The resulting residue was diluted with $CHCl_3$. The mixture was filtered through a $MgSO_4$ pad. The solution obtained was sequentially washed with HCl (aq 10%) and brine. The organic layer was dried over $MgSO_4$ and concentrated under vacuum to give crude **58**, which was further purified by silica flash column chromatography (hexanes/CH_2Cl_2, 1:4) to yield compound **58** (23 mg, 0.0094 mmol, 61%) as a yellow solid. Mp 98–99 °C; ^1H NMR ($CDCl_3$, 500 MHz) δ 10.04 (s, 2H), 7.91 (s, 2H), 7.88 (d, J=8.5 Hz, 4H), 7.81 (d, J=15.0 Hz, 2H), 7.69 (d, J=8.5 Hz, 4H), 7.60 (s, 4H), 7.55 (d, J=8.0 Hz, 2H), 7.48 (d, J=8.0 Hz, 4H), 7.41 (d, J=8 Hz, 2H), 7.28 (d, J=15.0 Hz, 2H), 7.07 (s, 2H), 7.06 (s, 4H), 7.04 (s, 2H), 6.87 (d, J=8.5 Hz, 4H), 4.09–4.02 (m, 16H), 3.83 (s, 6H), 1.92–1.17 (m, 128H), 0.89–0.82 (m, 24H). Meaningful ^{13}C NMR spectrum could not be obtained due to limited concentration; HRMS (MALDI-TOF) *m/z* calcd for $C_{170}H_{214}O_{12}$ 2447.6135, found 2448.8347 $[M+H]^+$.

Acknowledgements

This work was supported by the Natural Sciences and Engineering Research Council of Canada (NSERC) through the Discovery Grant program and Memorial University of Newfoundland. N.Z. thanks NSERC (PGS-D) for scholarship support.

Supplementary data

NMR spectroscopic data for all new compounds synthesized. Supplementary data associated with this article can be found in the online version, at doi:10.1016/j.tet.2010.11.012. These data include MOL files and InChIKeys of the most important compounds described in this article.

References and notes

1. Tour, J. M. *Acc. Chem. Res.* **2000**, *33*, 791–804.
2. Müllen, K.; Wegner, G. *Electronic Materials: The Oligomer Approach*; Wiley-VCH: Weinheim; New York, NY, 1998.
3. Brédas, J. L. *Conjugated Oligomers, Polymers, and Dendrimers: From Polyacetylene to DNA*; Bruxelles: Paris, 1999.
4. Martin, R. E.; Diederich, F. *Angew. Chem., Int. Ed.* **1999**, *38*, 1350–1377.
5. Grimsdale, A. C.; Müllen, K. *Angew. Chem., Int. Ed.* **2005**, *44*, 5592–5629.
6. Tour, J. M. *Chem. Rev.* **1996**, *96*, 537–554.
7. Meier, H. *Angew. Chem., Int. Ed.* **2005**, *44*, 2482–2506.
8. Thomas, S. W.; Joly, G. D.; Swager, T. M. *Chem. Rev.* **2007**, *107*, 1339–1386.
9. Müller, T. J. J.; Bunz, U. H. F. *Functional Organic Materials: Syntheses, Strategies and Applications*; Wiley-VCH: Weinheim, 2007.
10. Bunz, U. H. F. *Chem. Rev.* **2000**, *100*, 1605–1644.
11. Roncali, J. *Acc. Chem. Res.* **2000**, *33*, 147–156.
12. *Design and Synthesis of Conjugated Polymers*; Leclerc, M., Morin, J.-F., Eds.; Wiley-VCH: Weinheim, 2010.
13. Diederich, F.; Gobbi, L. In *Carbon Rich Compounds II, Macrocyclic Oligoacetylenes and Other Linearly Conjugated Systems*; de Meijere, A., Ed.; Springer: Berlin, 1999; pp 43–79.
14. Opsitnick, E.; Lee, D. *Chem.—Eur. J.* **2007**, *13*, 7040–7049.
15. Jiang, X.; Bollinger, J. C.; Lee, D. *J. Am. Chem. Soc.* **2006**, *128*, 11732–11733.
16. Tykwinski, R. R.; Zhao, Y. *Synlett* **2002**, *2002*, 1939–1953.
17. Kivala, M.; Mitzel, F.; Boudon, C.; Gisselbrecht, J. P.; Seiler, P.; Gross, M.; Diederich, F. *Chem.—Asian J.* **2006**, *1*, 479–489.
18. He, F.; Tian, L. L.; Tian, X. Y.; Xu, H.; Wang, Y. H.; Xie, W. J.; Hanif, M.; Xia, J. L.; Shen, F. Z.; Yang, B.; Li, F.; Ma, Y. G.; Yang, Y. Q.; Shen, J. C. *Adv. Funct. Mater.* **2007**, *17*, 1551–1557.
19. Pina, J.; Seixas de Melo, J.; Burrows, H. D.; Bilge, A.; Farrell, T.; Forster, M.; Scherf, U. *J. Phys. Chem. B* **2006**, *110*, 15100–15106.
20. Bilge, A.; Zen, A.; Forster, M.; Li, H.; Galbrecht, F.; Nehls, B. S.; Farrell, T.; Neher, D.; Scherf, U. *J. Mater. Chem.* **2006**, *16*, 3177–3182.
21. Zen, A.; Pingel, P.; Neher, D.; Scherf, U. *Phys. Stat. Sol.* **2008**, *205*, 440–448.
22. Sun, X. B.; Liu, Y. Q.; Chen, S. Y.; Qiu, W. F.; Yu, G.; Ma, Y. Q.; Qi, T.; Zhang, H. J.; Xu, X. J.; Zhu, D. B. *Adv. Funct. Mater.* **2006**, *16*, 917–925.
23. Zen, A.; Bilge, A.; Galbrecht, F.; Alle, R.; Meerholz, K.; Grenzer, J.; Neher, D.; Scherf, U.; Farrell, T. *J. Am. Chem. Soc.* **2006**, *128*, 3914–3915.
24. Al Ouahabi, A.; Baxter, P. N. W.; Gisselbrecht, J.-P.; De Cian, A.; Brelot, L.; Kyritsakas-Gruber, N. *J. Org. Chem.* **2009**, *74*, 4675–4689.
25. Kanibolotsky, A. L.; Berridge, R.; Skabara, P. J.; Perepichka, I. F.; Bradley, D. D. C.; Koeberg, M. *J. Am. Chem. Soc.* **2004**, *126*, 13695–13702.
26. Zhang, J.; Yang, Y.; He, C.; He, Y.; Zhao, G.; Li, Y. *Macromolecules* **2009**, *42*, 7619–7622.
27. Zen, A.; Pingel, P.; Jaiser, F.; Neher, D.; Grenzer, J.; Zhuang, W.; Rabe, J. P.; Bilge, A.; Galbrecht, F.; Nehls, B. S.; Farrell, T.; Scherf, U.; Abellon, R. D.; Grozema, F. C.; Siebbeles, L. D. A. *Chem. Mater.* **2007**, *19*, 1267–1276.
28. Mössinger, D.; Hornung, J.; Lei, S.; De Feyter, S.; Höger, S. *Angew. Chem., Int. Ed.* **2007**, *46*, 6802–6806.
29. Spitler, E. L.; Johnson, C. A.; Haley, M. M. *Chem. Rev.* **2006**, *106*, 5344–5386.
30. Godoy, J.; Vives, G.; Tour, J. M. *Org. Lett.* **2010**, *12*, 1464–1467.
31. Vives, G.; Kang, J.; Kelly, K. F.; Tour, J. M. *Org. Lett.* **2009**, *11*, 5602–5605.
32. Sasaki, T.; Osgood, A. J.; Alemany, L. B.; Kelly, K. F.; Tour, J. M. *Org. Lett.* **2007**, *10*, 229–232.
33. Sasaki, T.; Tour, J. M. *Org. Lett.* **2008**, *10*, 897–900.
34. Khatua, S.; Guerrero, J. M.; Claytor, K.; Vives, G.; Kolomeisky, A. B.; Tour, J. M.; Link, S. *ACS Nano* **2009**, *3*, 351–356.
35. Vives, G.; Tour, J. M. *Acc. Chem. Res.* **2009**, *42*, 473–487.
36. Shirai, Y.; Osgood, A. J.; Zhao, Y.; Kelly, K. F.; Tour, J. M. *Nano Lett.* **2005**, *5*, 2330–2334.
37. Shirai, Y.; Osgood, A. J.; Zhao, Y.; Yao, Y.; Saudan, L.; Yang, H.; Yu-Hung, C.; Alemany, L. B.; Sasaki, T.; Morin, J.-F.; Guerrero, J. M.; Kelly, K. F.; Tour, J. M. *J. Am. Chem. Soc.* **2006**, *128*, 4854–4864.
38. Miao, Q.; Chi, X.; Xiao, S.; Zeis, R.; Lefenfeld, M.; Siegrist, T.; Steigerwald, M. L.; Nuckolls, C. *J. Am. Chem. Soc.* **2006**, *128*, 1340–1345.
39. Klare, J. E.; Tulevski, G. S.; Sugo, K.; de Picciotto, A.; White, K. A.; Nuckolls, C. *J. Am. Chem. Soc.* **2003**, *125*, 6030–6031.
40. Grunder, S.; Huber, R.; Horhoiu, V.; González, M. T.; Schönenberger, C.; Calame, M.; Mayor, M. *J. Org. Chem.* **2007**, *72*, 8337–8344.
41. Florio, G. M.; Klare, J. E.; Pasamba, M. O.; Werblowsky, T. L.; Hyers, M.; Berne, B. J.; Hybertsen, M. S.; Nuckolls, C.; Flynn, G. W. *Langmuir* **2006**, *22*, 10003–10008.

42. Pham, P.-T. T.; Xia, Y.; Frisbie, C. D.; Bader, M. M. *J. Phys. Chem. C* **2008**, *112*, 7968–7971.
43. Jiang, X.; Gyu Park, B.; Riddle, J. A.; June Zhang, B.; Pink, M.; Lee, D. *Chem. Commun.* **2008**, 6028–6030.
44. Sonntag, M.; Kreger, K.; Hanft, D.; Strohriegl, P.; Setayesh, S.; de Leeuw, D. *Chem. Mater.* **2005**, *17*, 3031–3039.
45. Diring, S. p.; Puntoriero, F.; Nastasi, F.; Campagna, S.; Ziessel, R. *J. Am. Chem. Soc.* **2009**, *131*, 6108–6110.
46. Brombosz, S. M.; Zucchero, A. J.; Phillips, R. L.; Vazquez, D.; Wilson, A.; Bunz, U. H. F. *Org. Lett.* **2007**, *9*, 4519–4522.
47. Zucchero, A. J.; Wilson, J. N.; Bunz, U. H. F. *J. Am. Chem. Soc.* **2006**, *128*, 11872–11881.
48. Zucchero, A. J.; McGrier, P. L.; Bunz, U. H. F. *Acc. Chem. Res.* **2010**, *43*, 397–408.
49. Tolosa, J.; Zucchero, A. J.; Bunz, U. H. F. *J. Am. Chem. Soc.* **2008**, *130*, 6498–6506.
50. Wilson, J. N.; Bunz, U. H. F. *J. Am. Chem. Soc.* **2005**, *127*, 4124–4125.
51. Marsden, J. A.; Miller, J. J.; Shirtcliff, L. D.; Haley, M. M. *J. Am. Chem. Soc.* **2005**, *127*, 2464–2476.
52. McGrier, P. L.; Solntsev, K. M.; Schonhaber, J.; Brombosz, S. M.; Tolbert, L. M.; Bunz, U. H. F. *Chem. Commun.* **2007**, 2127–2129.
53. Sùrensen, J. K.; Vestergaard, M.; Kadziola, A.; Kilså, K.; Nielsen, M. B. *Org. Lett.* **2006**, *8*, 1173–1176.
54. Guthrie, D. A.; Tovar, J. D. *Org. Lett.* **2008**, *10*, 4323–4326.
55. Dalton, G. T.; Cifuentes, M. P.; Petrie, S.; Stranger, R.; Humphrey, M. G.; Samoc, M. *J. Am. Chem. Soc.* **2007**, *129*, 11882–11883.
56. Zhang, H. C.; Guo, E. Q.; Zhang, Y. L.; Ren, P. H.; Yang, W. J. *Chem. Mater.* **2009**, *21*, 5125–5135.
57. Tolosa, J.; Solntsev, K. M.; Tolbert, L. M.; Bunz, U. H. F. *J. Org. Chem.* **2009**, *75*, 523–534.
58. Grunder, S.; Huber, R.; Wu, S.; Schönenberger, C.; Calame, M.; Mayor, M. *Eur. J. Org. Chem.* **2010**, *2010*, 833–845.
59. Cui, W.; Fu, Y.; Qu, Y.; Tian, H.; Zhang, J.; Xie, Z.; Geng, Y.; Wang, F. *Chem.—Asian J.* **2010**, *5*, 932–940.
60. Sun, J.; Cheng, J. G.; Zhu, W. Q.; Ren, S. J.; Zhong, H. L.; Zeng, D. L.; Du, J. P.; Xu, E. J.; Liu, Y. C.; Fang, Q. *J. Polym. Sci., Part A: Polym. Chem.* **2008**, *46*, 5616–5625.
61. Zhou, N.; Wang, L.; Thompson, D. W.; Zhao, Y. *Tetrahedron Lett.* **2007**, *48*, 3563–3567.
62. Winter, A.; Friebe, C.; Hager, M. D.; Schubert, U. S. *Eur. J. Org. Chem.* **2009**, *2009*, 801–809.
63. Cherioux, F.; Audebert, P.; Hapiot, P. *Chem. Mater.* **1998**, *10*, 1984–1989.
64. Kannan, R.; He, G. S.; Lin, T.-C.; Prasad, P. N.; Vaia, R. A.; Tan, L.-S. *Chem. Mater.* **2003**, *16*, 185–194.
65. Omer, K. M.; Ku, S.-Y.; Chen, Y.-C.; Wong, K.-T.; Bard, A. J. *J. Am. Chem. Soc.* **2010**, *132*, 10944–10952.
66. Wang, J.-L.; Tang, Z.-M.; Xiao, Q.; Ma, Y.; Pei, J. *Org. Lett.* **2009**, *11*, 863–866.
67. Nicolas, Y.; Blanchard, P.; Levillain, E.; Allain, M.; Mercier, N.; Roncali, J. *Org. Lett.* **2003**, *6*, 273–276.
68. Zhou, X.-H.; Yan, J.-C.; Pei, J. *Org. Lett.* **2003**, *5*, 3543–3546.
69. Ma, Z.; Wang, Y.-Y.; Wang, P.; Huang, W.; Li, Y.-B.; Lei, S.-B.; Yang, Y.-L.; Fan, X.-L.; Wang, C. *ACS Nano* **2007**, *1*, 160–167.
70. Yang, J.-S.; Huang, H.-H.; Ho, J.-H. *J. Phys. Chem. B* **2008**, *112*, 8871–8878.
71. Tang, Z.-M.; Lei, T.; Wang, J.-L.; Ma, Y.; Pei, J. *J. Org. Chem.* **2010**, *75*, 3644–3655.
72. Yang, J.-S.; Huang, H.-H.; Liu, Y.-H.; Peng, S.-M. *Org. Lett.* **2009**, *11*, 4942–4945.
73. Justin Thomas, K. R.; Lin, J. T.; Tao, Y.-T.; Ko, C.-W. *Chem. Mater.* **2002**, *14*, 1354–1361.
74. Yang, J.-S.; Lee, Y.-R.; Yan, J.-L.; Lu, M.-C. *Org. Lett.* **2006**, *8*, 5813–5816.
75. Cui, Y.; Wang, S. *J. Org. Chem.* **2006**, *71*, 6485–6496.
76. Taerum, T.; Lukoyanova, O.; Wylie, R. G.; Perepichka, D. F. *Org. Lett.* **2009**, *11*, 3230–3233.
77. Jia, H.-P.; Liu, S.-X.; Sanguinet, L.; Levillain, E.; Decurtins, S. *J. Org. Chem.* **2009**, *74*, 5727–5729.
78. Zhang, W.-B.; Jin, W.-H.; Zhou, X.-H.; Pei, J. *Tetrahedron* **2007**, *63*, 2907–2914.
79. Sharma, A.; Sharma, N.; Kumar, R.; Shard, A.; Sinha, A. K. *Chem. Commun.* **2010**, *46*, 3283–3285.
80. Arrigoni, C.; Schull, G.; Blećger, D.; Douillard, L.; Fiorini-Debuisschert, C. l.; Mathevet, F.; Kreher, D.; Attias, A.-J.; Charra, F. *J. Phys. Chem. Lett.* **2009**, *1*, 190–194.
81. Shirai, Y.; Zhao, Y.; Cheng, L.; Tour, J. M. *Org. Lett.* **2004**, *6*, 2129–2132.
82. Zhou, N.; Zhao, Y. *J. Org. Chem.* **2010**, *75*, 1498–1516.
83. Zhao, Y.; Shirai, Y.; Slepkov, A. D.; Cheng, L.; Alemany, L. B.; Sasaki, T.; Hegmann, F. A.; Tour, J. M. *Chem.—Eur. J.* **2005**, *11*, 3643–3658.
84. Chandra, K. L.; Zhang, S.; Gorman, C. B. *Tetrahedron* **2007**, *63*, 7120–7132.
85. Zhou, N.; Wang, L.; Thompson, D. W.; Zhao, Y. *Org. Lett.* **2008**, *10*, 3001–3004.
86. Kong, Q.; Zhu, D.; Quan, Y.; Chen, Q.; Ding, J.; Lu, J.; Tao, Y. *Chem. Mater.* **2007**, *19*, 3309–3318.
87. Nierengarten, J.-F.; Zhang, S.; Gégout, A.; Urbani, M.; Armaroli, N.; Marconi, G.; Rio, Y. *J. Org. Chem.* **2005**, *70*, 7550–7557.
88. Le, Z.-G.; Chen, Z.-C.; Hu, Y.; Zheng, Q.-G. *Synthesis* **2004**, *2004*, 2809–2812.
89. Frahn, J.; Schlüter, A. D. *Synthesis* **1997**, *1997*, 1301–1304.
90. Cade, I.; Long, N. J.; White, A. J. P.; Williams, D. J. *J. Organomet. Chem.* **2006**, *691*, 1389–1401.
91. Lv, X.; Mao, J.; Liu, Y.; Huang, Y.; Ma, Y.; Yu, A.; Yin, S.; Chen, Y. *Macromolecules* **2008**, *41*, 501–503.
92. Ranganathan, A.; Heisen, B. C.; Dix, I.; Meyer, F. *Chem. Commun.* **2007**, 3637–3639.
93. Wolska, J.; Mieczkowski, J.; Pociecha, D.; Buathong, S. w.; Donnio, B.; Guillon, D.; Gorecka, E. *Macromolecules* **2009**, *42*, 6375–6384.
94. Binstead, R.A.; Zuberbühler, A.D. Spectrum Software Associates: Chapel Hill, NC, 1993–1997.